AD-A072 751 PURDUE UNIV LAFAYETTE IN SCHOOL OF ELECTRICAL ENGINEERING F/G 17/9
SPACE-TIME SIGNAL PROCESSING OF RADAR RETURNS.(U)
JUN 79 G R COOPER, C D MCGILLEM F30602-75-C-0082

UNCLASSIFIED RADC-TR-79-156 NL

| OF |
AD A072751

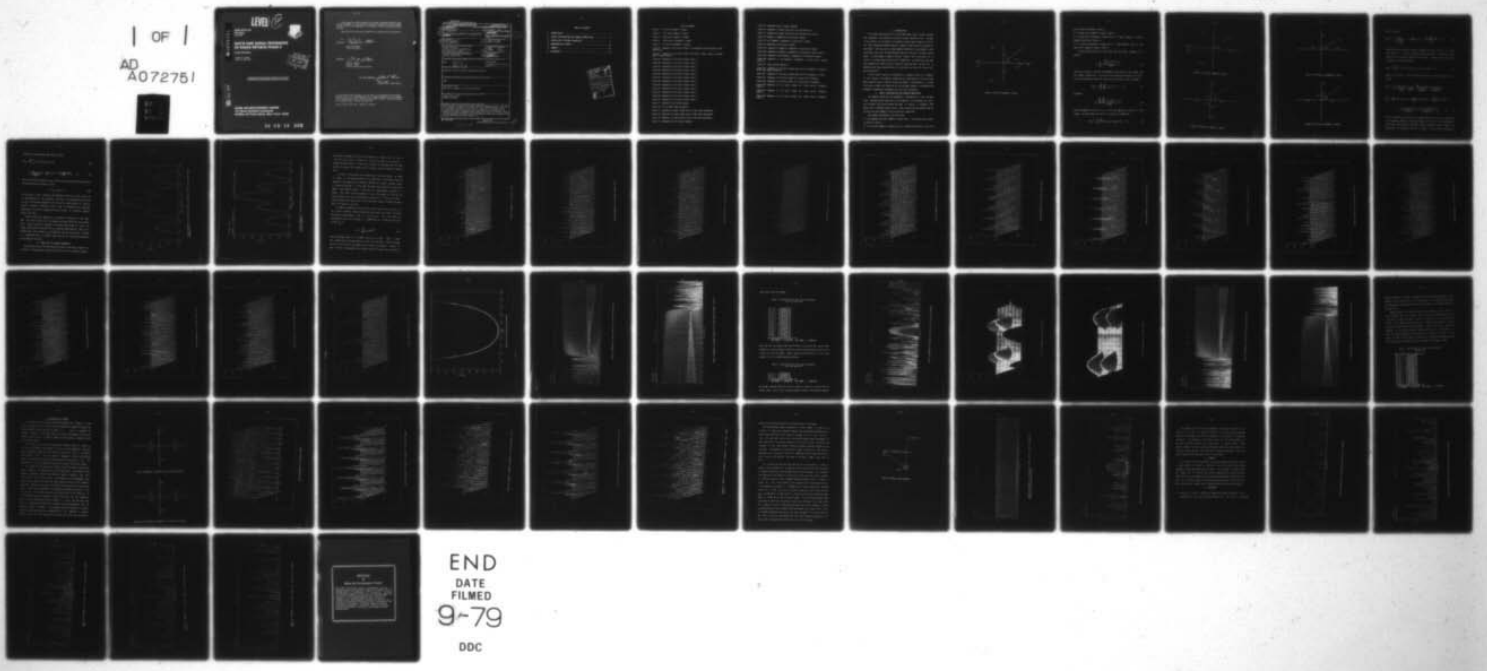

END
DATE FILMED
9-79
DDC

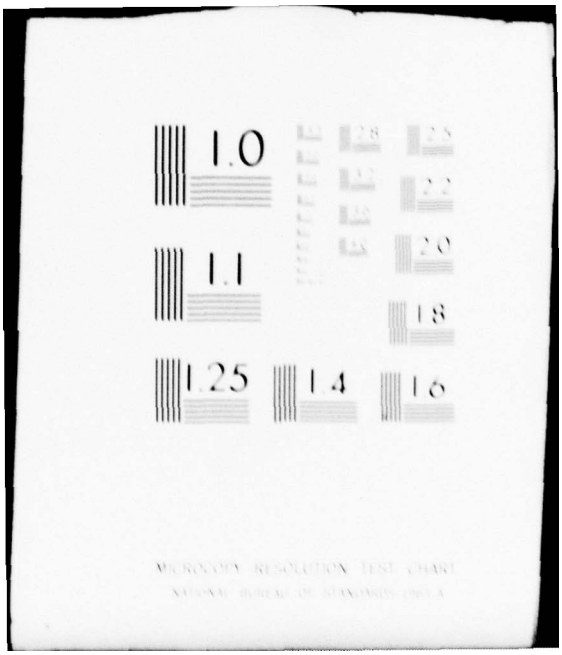
1.0
1.1
1.25
1.4
1.6
2.0
2.2
2.5
MICROCOPY RESOLUTION TEST CHART
NATIONAL BUREAU OF STANDARDS 1963-A

LEVEL II

RADC-TR-79-156
Phase Report
June 1979

SPACE-TIME SIGNAL PROCESSING OF RADAR RETURNS PHASE II

Purdue University

George R. Cooper
Clare D. McGillem

ROME AIR DEVELOPMENT CENTER
Air Force Systems Command
Griffiss Air Force Base, New York 13441

This report has been reviewed by the RADC Information Office (OI) and is releasable to the National Technical Information Service (NTIS). At NTIS it will be releasable to the general public, including foreign nations.

RADC-TR-79-156 has been reviewed and is approved for publication.

APPROVED: Paul Van Etten

PAUL VAN ETTEN
Project Engineer

APPROVED: Owen R. Lawter

OWEN R. LAWTER
Colonel, USAF
Chief, Surveillance Division

FOR THE COMMANDER: John P. Huss

JOHN P. HUSS
Acting Chief, Plans Office

If your address has changed or if you wish to be removed from the RADC mailing list, or if the addressee is no longer employed by your organization, please notify RADC (OCTS) Griffiss AFB NY 13441. This will assist us in maintaining a current mailing list.

Do not return this copy. Retain or destroy.

AD55758

UNCLASSIFIED

SECURITY CLASSIFICATION OF THIS PAGE (When Data Entered)

REPORT DOCUMENTATION PAGE

READ INSTRUCTIONS BEFORE COMPLETING FORM

1. REPORT NUMBER: RADC-TR-79-156	2. GOVT ACCESSION NO.
3. RECIPIENT'S CATALOG NUMBER: Rept. for
4. TITLE (and Subtitle): SPACE-TIME SIGNAL PROCESSING OF RADAR RETURNS. PHASE II	5. TYPE OF REPORT & PERIOD COVERED: Phase Report, Dec 77—Oct 78 and Phase 2.
	6. PERFORMING ORG. REPORT NUMBER: N/A
7. AUTHOR(s): George R. Cooper, Clare D. McGillem	8. CONTRACT OR GRANT NUMBER(s): F30602-75-C-0082
9. PERFORMING ORGANIZATION NAME AND ADDRESS: Purdue University, School of Electrical Engineering, W. Lafayette IN 47907	10. PROGRAM ELEMENT, PROJECT, TASK AREA & WORK UNIT NUMBERS: 62702F, 95670015, 00
11. CONTROLLING OFFICE NAME AND ADDRESS: Rome Air Development Center (OCTS), Griffiss AFB NY 13441	12. REPORT DATE: June 1979
	13. NUMBER OF PAGES: 58
14. MONITORING AGENCY NAME & ADDRESS (if different from Controlling Office): Same (12 54p.)	15. SECURITY CLASS. (of this report): UNCLASSIFIED
	15a. DECLASSIFICATION DOWNGRADING SCHEDULE: N/A

16. DISTRIBUTION STATEMENT (of this Report)

Approved for public release; distribution unlimited.

17. DISTRIBUTION STATEMENT (of the abstract entered in Block 20, if different from Report)

Same

18. SUPPLEMENTARY NOTES

RADC Project Engineer: Paul Van Etten (OCTS)

19. KEY WORDS (Continue on reverse side if necessary and identify by block number)

Target cross section
Signal Processing

20. ABSTRACT (Continue on reverse side if necessary and identify by block number)

This work shows the presence of spatial symmetries which may allow a radar system to predict a frequency which will give a near maximum response as the target approaches the radar. If the target is complex then the target may be resolved into simpler components, which have desirable characteristics, and symmetries that may be expolited when tracking the target. An efficient method for the approximate evaluation of the time ambiguity functions for complex pulse envelope shapes has also been presented.

DD FORM 1 JAN 73 1473

UNCLASSIFIED

SECURITY CLASSIFICATION OF THIS PAGE (When Data Entered)

292 900

TABLE OF CONTENTS

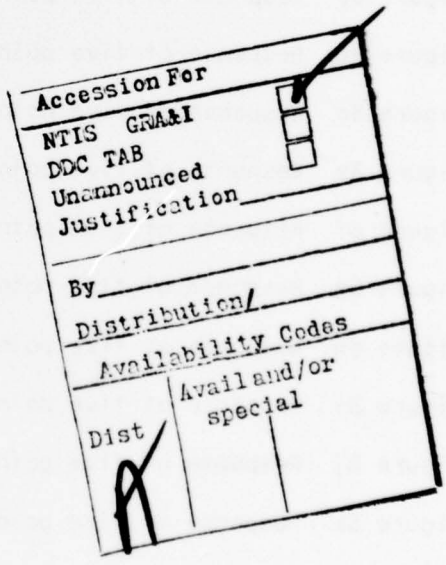

LIST OF FIGURES

1. INTRODUCTION

This report describes work on the optimum radar signal design problem and represents an extension of previous studies reported in [1]. The goal of this project is the design of an adaptive radar signal capable of providing near optimum performance against a complex target having a changing aspect angle. Previous work included computer modeling of performance using continuous wave and pulsed waveforms against a ten point reflector target model. A large number of sample received signals were calculated for a variety of azimuth angles and carrier frequencies. In addition to the computer modeling of radar returns an analytic study has been carried out to determine the signal waveform that will maximize the return for a given target orientation.

In this report results are presented of a computer search for symmetry in the returns from complex targets and an investigation of how such symmetry might be used to improve system performance. Performance of a system utilizing an empirical prediction of the optimum frequency is presented and methods of breaking up nonsymmetrical pairs are considered.

2. TARGET CONFIGURATIONS AND PROBLEM FORMULATION

The computer simulation was expanded by implementing a near optimum pulse envelope and by searching for any symmetry in the response as a function of angle, which would enable the radar to predict a frequency that would give a maximum signal return. Also, targets were considered that do not have the even symmetry that the 10 point target had.

The targets considered in this work are:

1) The standard ten point symmetric target used in the previous work, which is shown in Figure 1.

2) A five point symmetric target, which is a simplified version of the ten

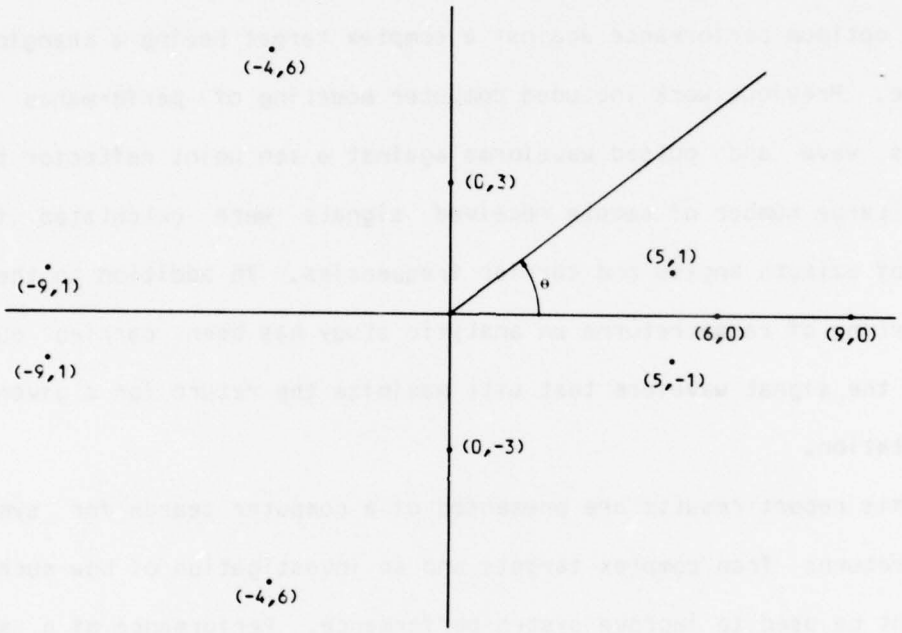

Figure 1 Ten point symmetric target.

point target used before, Figure 2.

3) An eight point symmetric target, Figure 3.

4) A three point nonsymmetric target, which is simple enough to explore symmetry generation, Figure 4.

5) A six point nonsymmetric target, which is approximately half of the eight point symmetric target, Figure 5.

In the previous work [1], it was shown that the target response R is given by

$$R = \frac{E_d}{E_0} = \frac{\int_{-2T}^{2T} R_e(\tau)\, R_h(\tau)\, d\tau}{R_e(0)} \tag{1}$$

where $R_e(\tau)$ and $R_h(\tau)$ are the time ambiguity functions for the signal and the target, respectively. Since we are considering the target as a collection of M reflectors, each with reflection coefficient a_i, $R_h(\tau)$ becomes

$$R_h(\tau) = \sum_{i=1}^{M} \sum_{j=1}^{M} a_i\, a_j\, \delta(T + \tau_i - \tau_j) \tag{2}$$

R becomes

$$R = \frac{\sum_{i=1}^{M} \sum_{j=1}^{M} a_i\, a_j\, R_e(\tau_i - \tau_j)}{R_e(0)} \tag{3}$$

and the response is a function only of the time ambiguity function of the signal. For an RF pulse the ambiguity function is defined as

$$R_e(\tau) = \int_{-T}^{T-\tau} \frac{E_0}{T} \cos \omega_0 t \cos \omega_0 (t+\tau) d\tau \qquad \tau > 0 \tag{4}$$

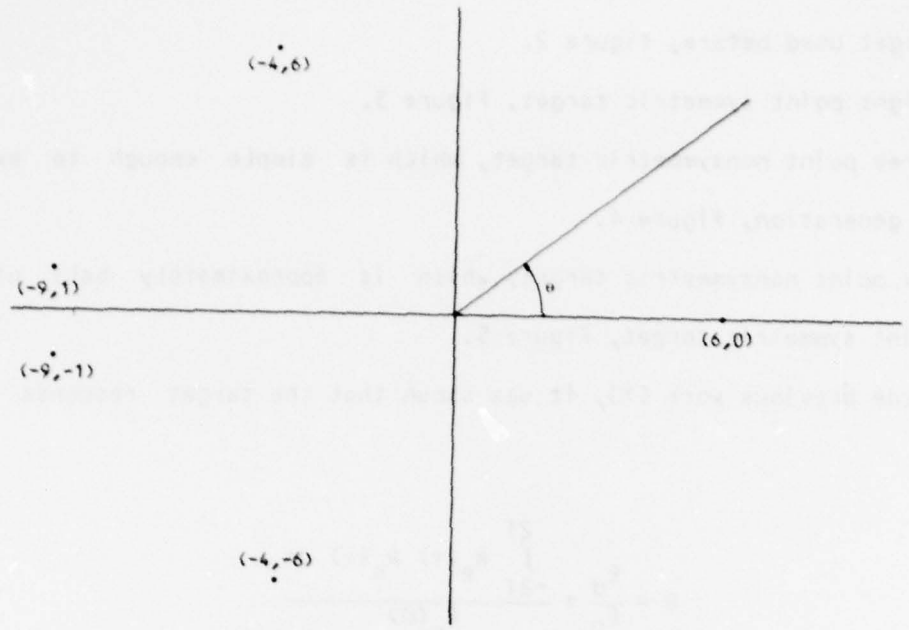

Figure 2 Five point symmetric target.

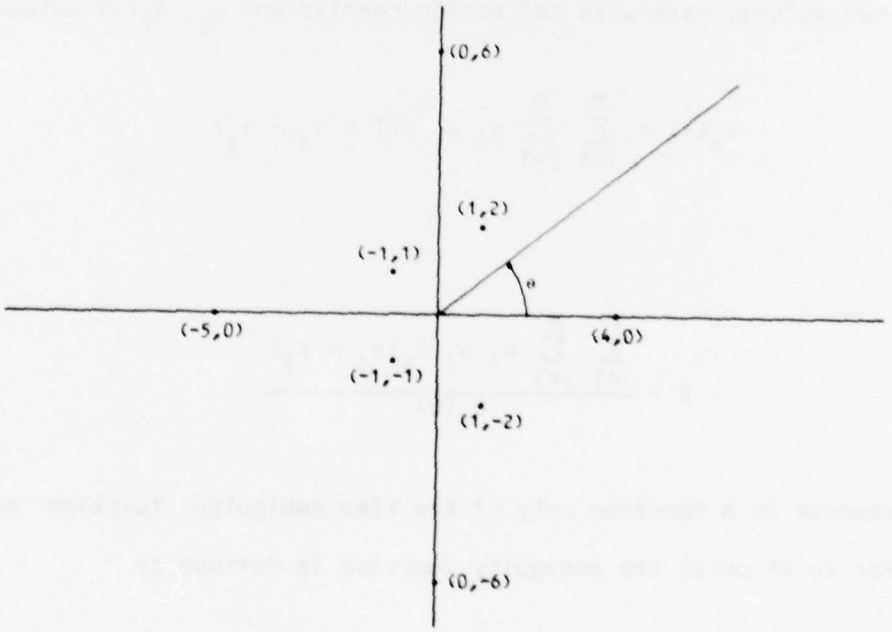

Figure 3 Eight point symmetric target.

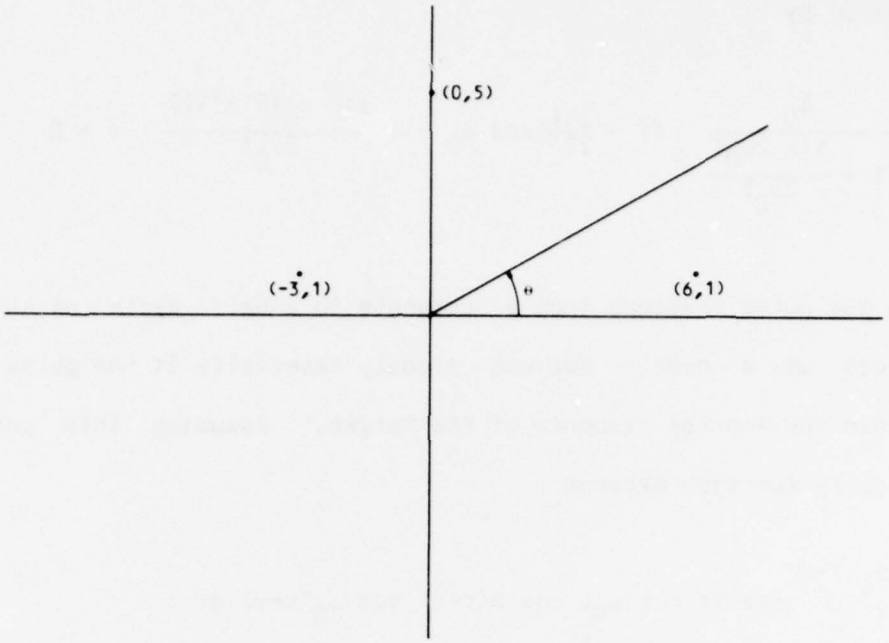

Figure 4 Three point nonsymmetric target.

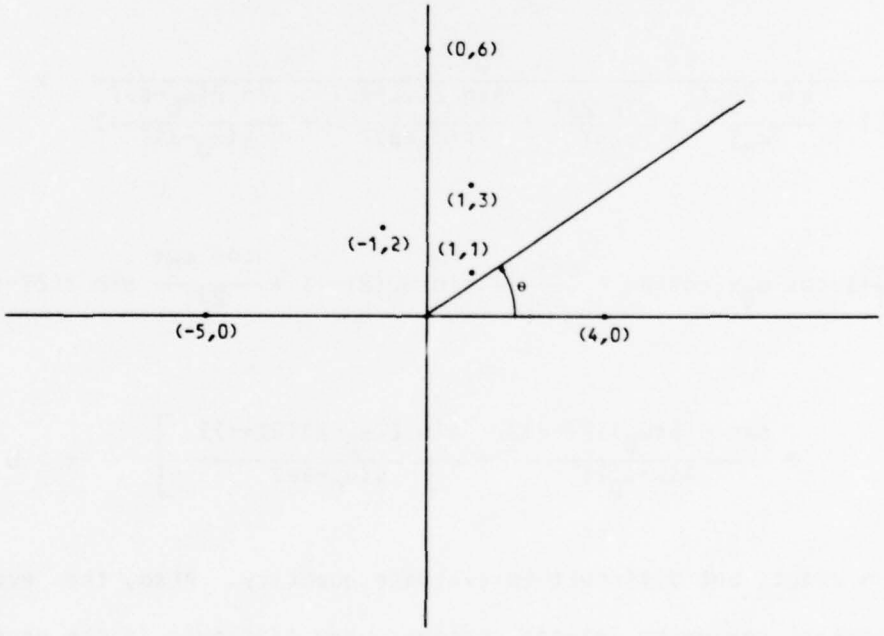

Figure 5 Six point nonsymmetric target.

and is given by

$$R_e(\tau) = \frac{E_0}{1 + \frac{\sin 2\omega_0 T}{2\omega_0 T}} \left(1 - \frac{|\tau|}{2T}\right)\cos \omega_0 \tau + \frac{\sin \omega_0(2T-|\tau|)}{2\omega_0 T} \qquad \tau > 0 \qquad (5)$$

Changing the pulse envelope from a rectangle to a half cycle of a cosine wave gives us a nearly optimum signal, especially if the pulse is much longer than the impulse response of the target. Assuming this condition, the ambiguity function becomes

$$R_e(\tau) = \frac{E_0}{T} \int_{-T}^{T-\tau} \cos \beta t \cos \omega_0 t \cos \beta(t+\tau) \cos \omega_0(t+\tau)\, d\tau \qquad (6)$$

where $\beta T = \pi/2$ and $T = 1/2$ of the RF pulse duration. Upon integration this yields

$$R_e(\tau) = \frac{E_0}{\left[1 + \frac{\sin 2\omega_0 T}{2\omega_0 T} + \frac{\sin 2\beta T}{2\beta T} + \frac{\sin 2(\omega_0+\beta)T}{4(\omega_0+\beta)T} + \frac{\sin 2(\omega_0-\beta)T}{4(\omega_0-\beta)T}\right]} \times$$

$$\left[\left(1 - \frac{|\tau|}{2T}\right) \cos \omega_0 \tau \cos \beta\tau + \frac{\cos \beta\tau}{2\omega_0 T} \sin \omega_0(2T-\tau) + \frac{\cos \omega_0 \tau}{2\beta T} \sin \beta(2T-\tau) \right.$$

$$\left. + \frac{\sin [(\beta+\omega_0)(2T-\tau)]}{4(\beta+\omega_0)T} + \frac{\sin [(\omega_0-\beta)(2T-\tau)]}{4(\omega_0-\beta)T} \right] \qquad \tau > 0 \qquad (7)$$

This is an exact, but difficult to evaluate quantity. Also, the evaluation of the general ambiguity integral becomes very difficult if the envelope is other than a simple shape. Because of these problems another method for evaluating the ambiguity function is needed. If we consider the ambiguity

function of the envelope shape alone, we get

$$R(\tau) = \frac{E_0}{T} \int_{-T}^{T-\tau} \cos \beta t \cos \beta(t+\tau)\, dt \tag{8}$$

$$= \frac{E_0}{1 + \frac{\sin 2\beta T}{2\beta T}} \left[\left(1 - \frac{(\tau)}{2T}\right) \cos \beta\tau + \frac{\sin \beta(2T-(\tau)}{2\beta T} \right] \quad \tau > 0 \tag{9}$$

which can be multiplied by cos $\omega_0 t$ to give the two more significant terms of the previous exact expression, since

$$\beta + \omega_0 > \omega_0 - \beta >> \beta \tag{10}$$

if the pulse is long. Therefore, the ambiguity function of a RF pulse can be approximated by the ambiguity function of its envelope multiplied by cos $\omega_0 t$. The envelope ambiguity function can be approximated by discrete Fourier transform techniques, that allows the consideration of envelope shapes which can not be integrated directly as well as providing computational efficiency.

Figure 6 shows the response, as a function of frequency, of the standard ten point target to the rectangular RF pulse using the exact expression. Figure 7 shows the response of the same target using the cosine envelope pulse and the discrete Fourier transform approximation. Both curves reached their local maxima at f_c=4.45165 GHz, but the cosine pulse attained R = 19.585 dB, which is slightly larger than the R = 19.455 dB attained by the rectangular RF pulse.

3. PREDICTION OF OPTIMUM FREQUENCIES

In previous work we have seen detailed views of the target response as a function of both angle of observation and of carrier frequency; however,

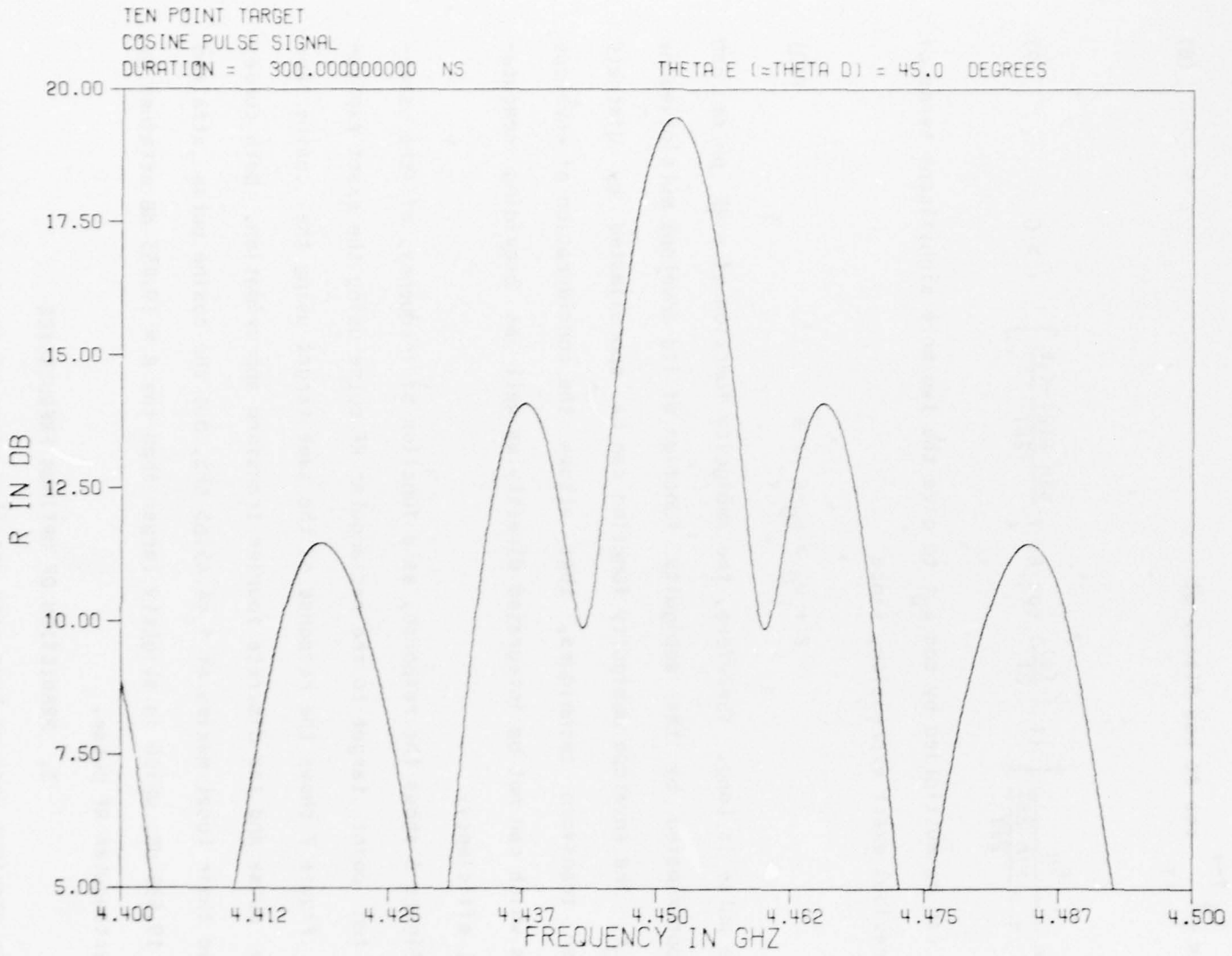

Figure 6 Response of ten point target to rectangular RF pulse using exact expression.

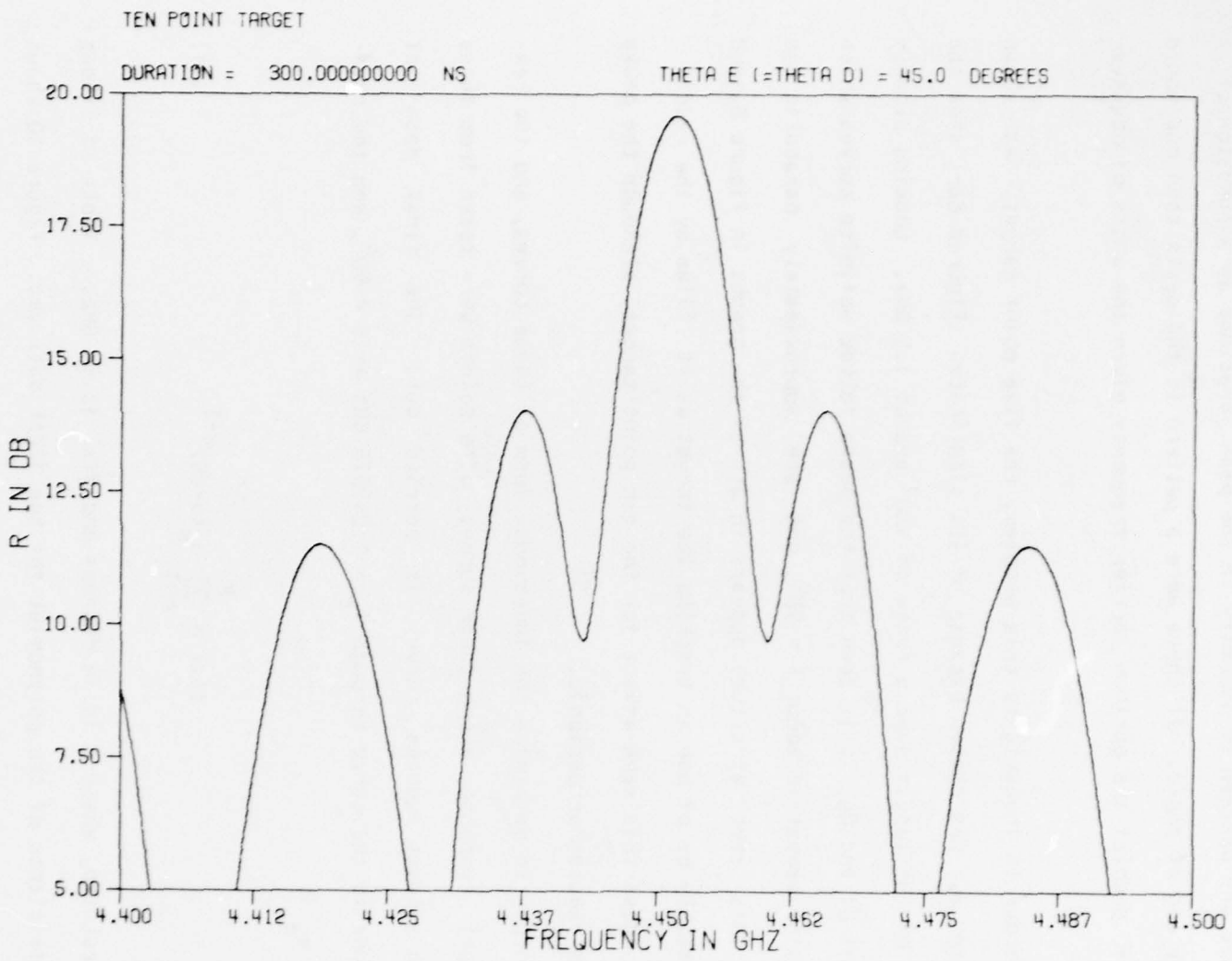

Figure 7 Response of ten point target to RF pulse using cosine envelope and DFT approximation.

there was no attempt to look at the response on a large scale to see if there were any pattern or symmetry in the peak locations as a function of frequency and of angle. If there were a pattern to the peaks then one would be able to predict the optimum carrier frequency given the angle of observation.

In order to investigate this problem, the five point target, as shown in Figure 2, was chosen because of its simplicity. Figures 8a-l show the response of the target over a range of 120^{o} and of 1.5 GHz. Looking closely at Figures 8f and 8g, it is seen that the peaks follow definite curves which appear to be symmetric about $\theta = 90^{o}$, and are approximately parabolic in shape. This same structure appears in all of the graphs in Figure 8, and could possibly be of use in tracking the target as it flies by the radar. Figure 9 shows this same effect for the ten point target, although the peaks aren't as regular or periodic.

In order to determine the functional form of these curves, and the exact target response along these curves, data points were taken from these plots and a least squares curve fit carried out. The first data set corresponds to the curve through $f_c = 1.049375$ GHz at $\theta = 90^{o}$, and the coefficients a_m in

$$f(x) = \sum_{m=1}^{M} a_m (x-90)^{m-1} \qquad (11)$$

were calculated, where x is in degrees and f(x) is in GHz. Table 1 shows the coefficients of the polynomial for the first data set. Figure 10 shows the fit of the curve to the sample points, shown as triangles. Figures 11 and 12 show the response of the target along this curve, the way that the

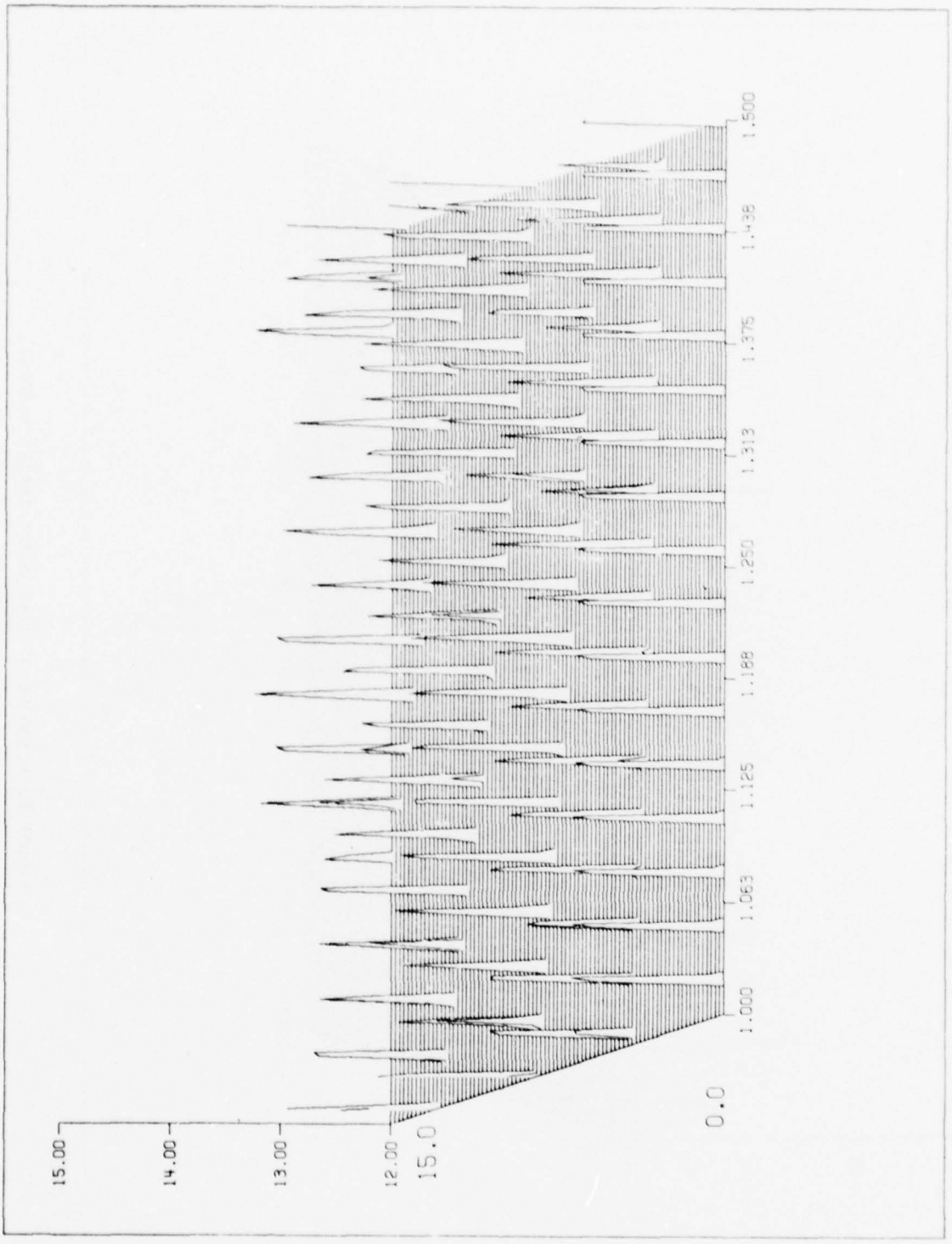

Figure 8a Response of five point target.

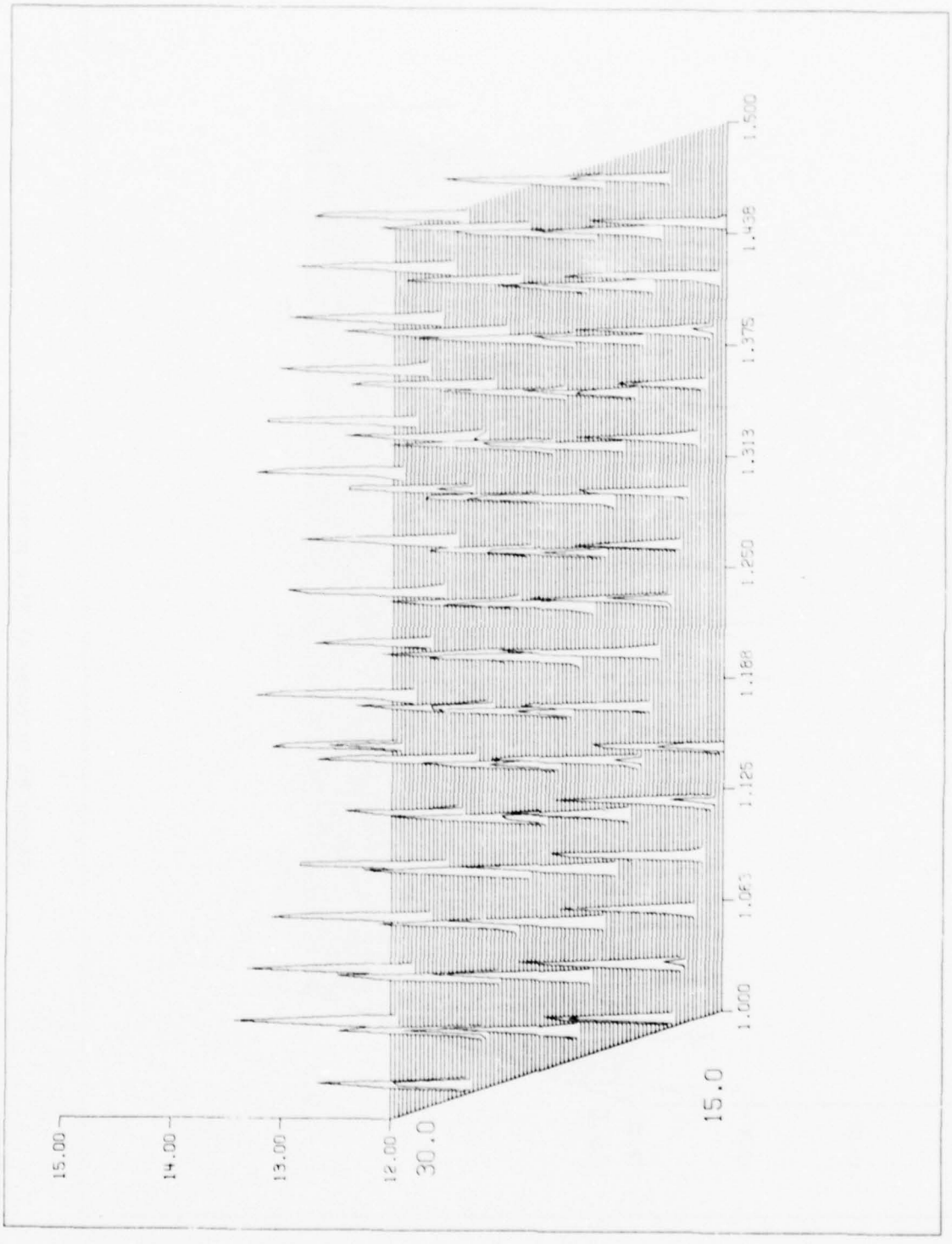

Figure 8b Response of five point target (cont.).

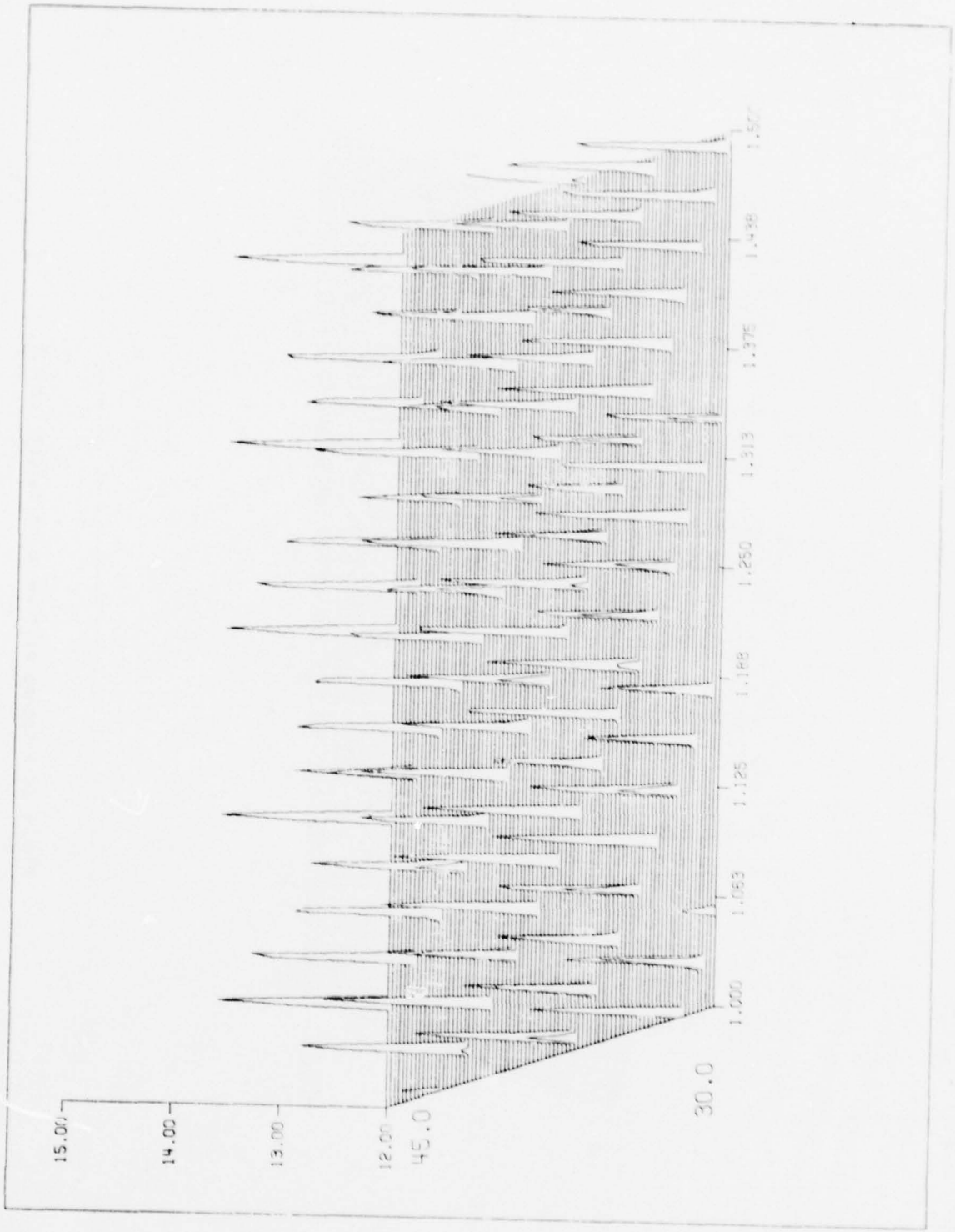

Figure 8c Response of five point target (cont.).

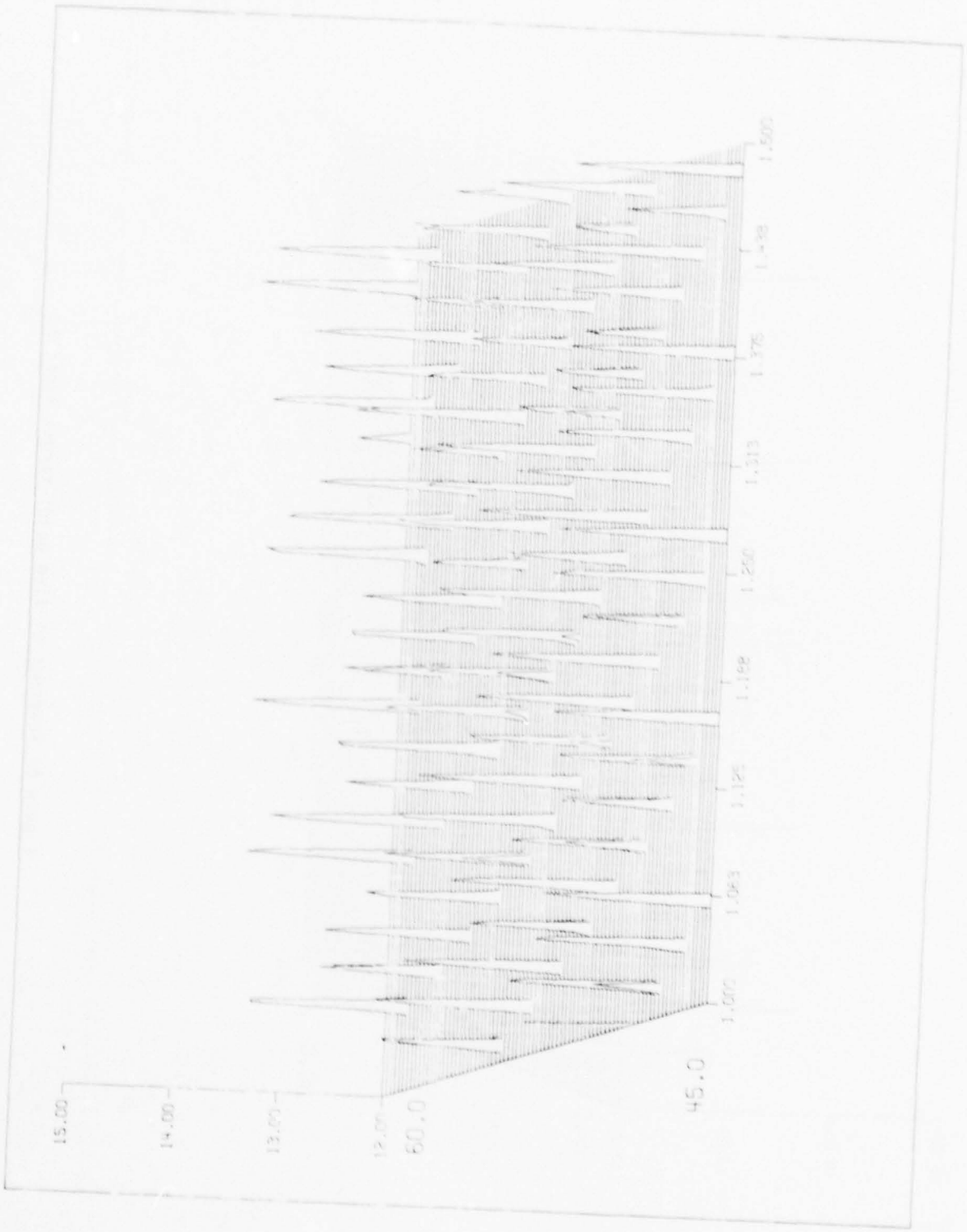

Figure 8a Response of five point target (cont.).

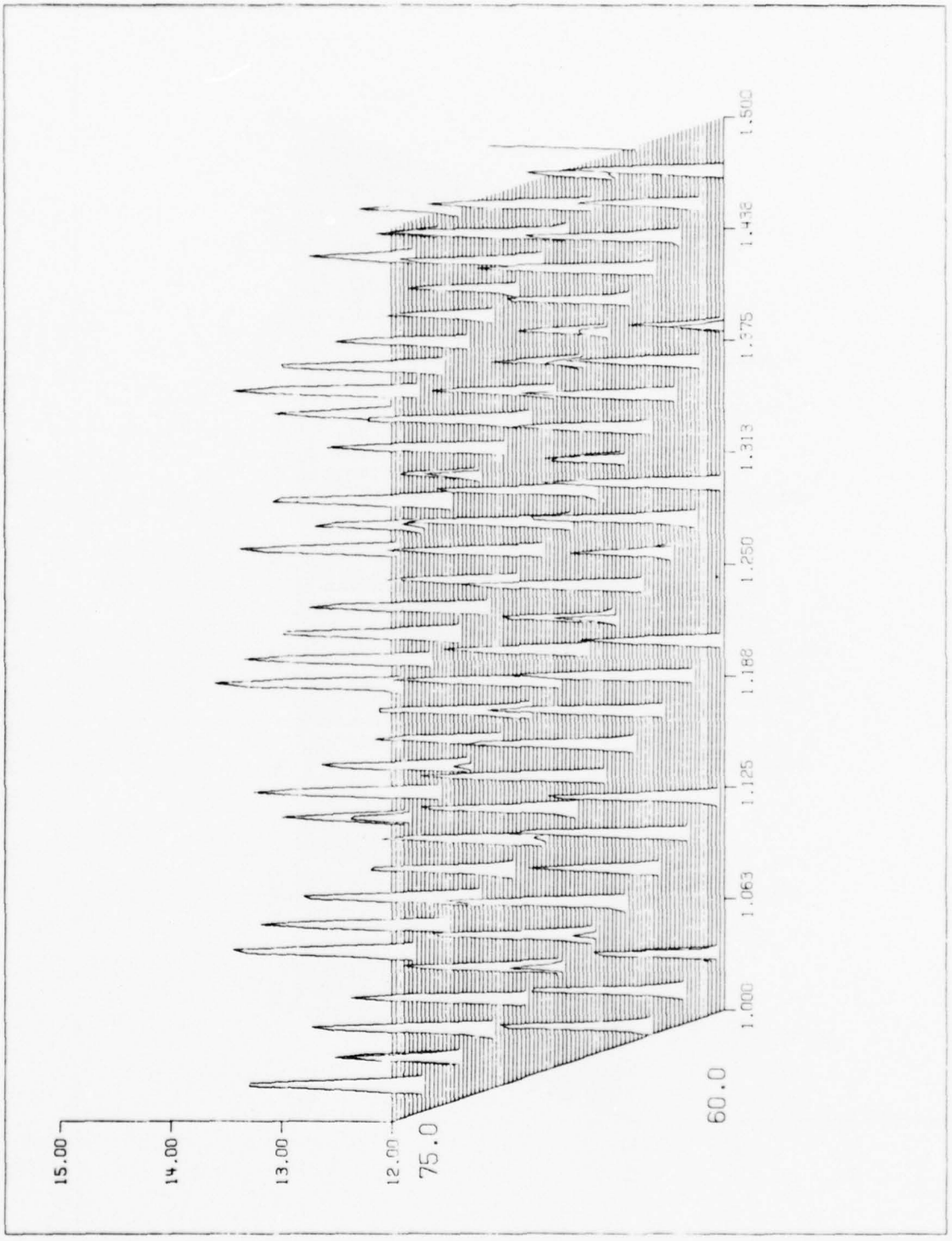

Figure 8e Response of five point target (cont.).

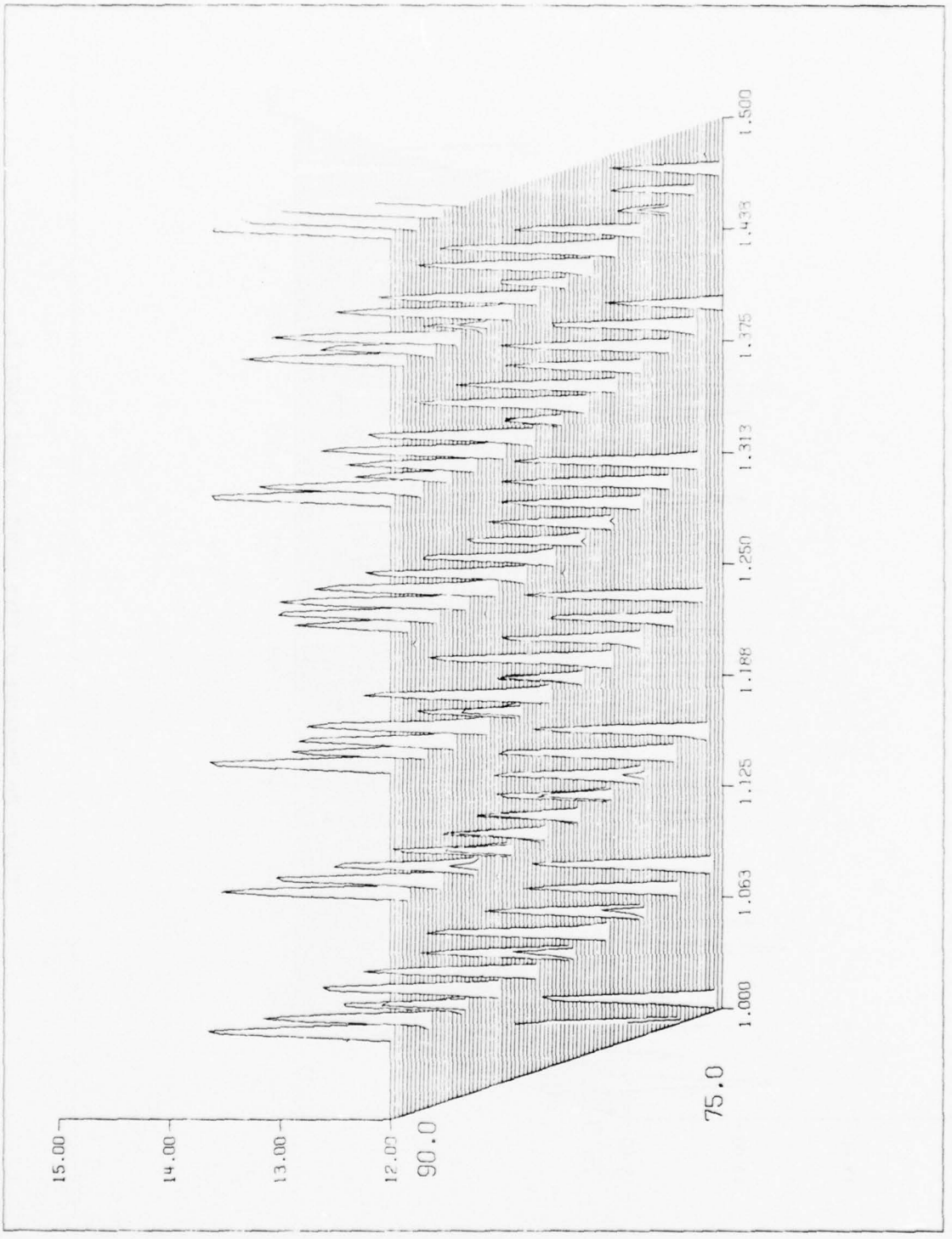

Figure 8f Response of five point target (cont.).

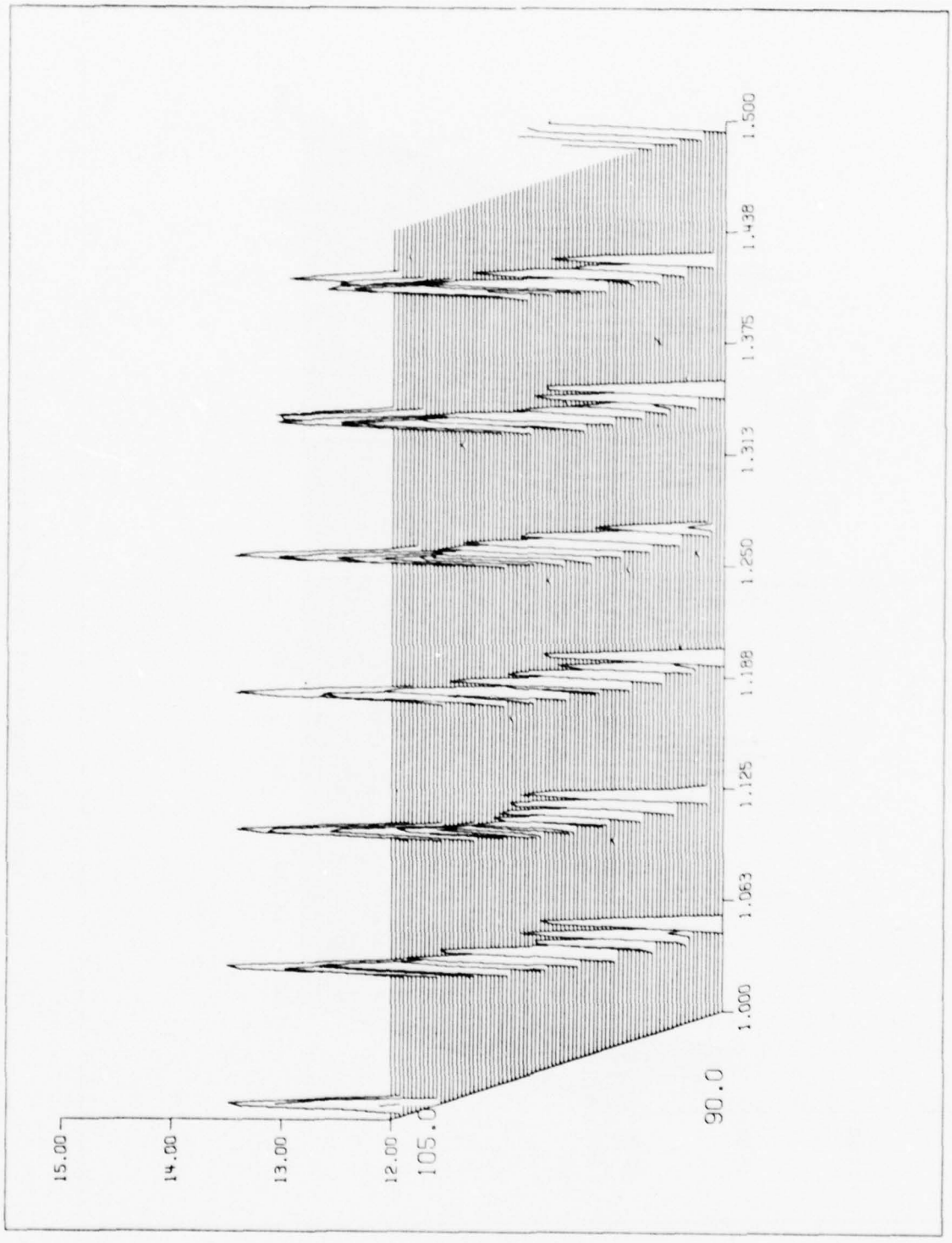

Figure 8g Response of five point target (cont.).

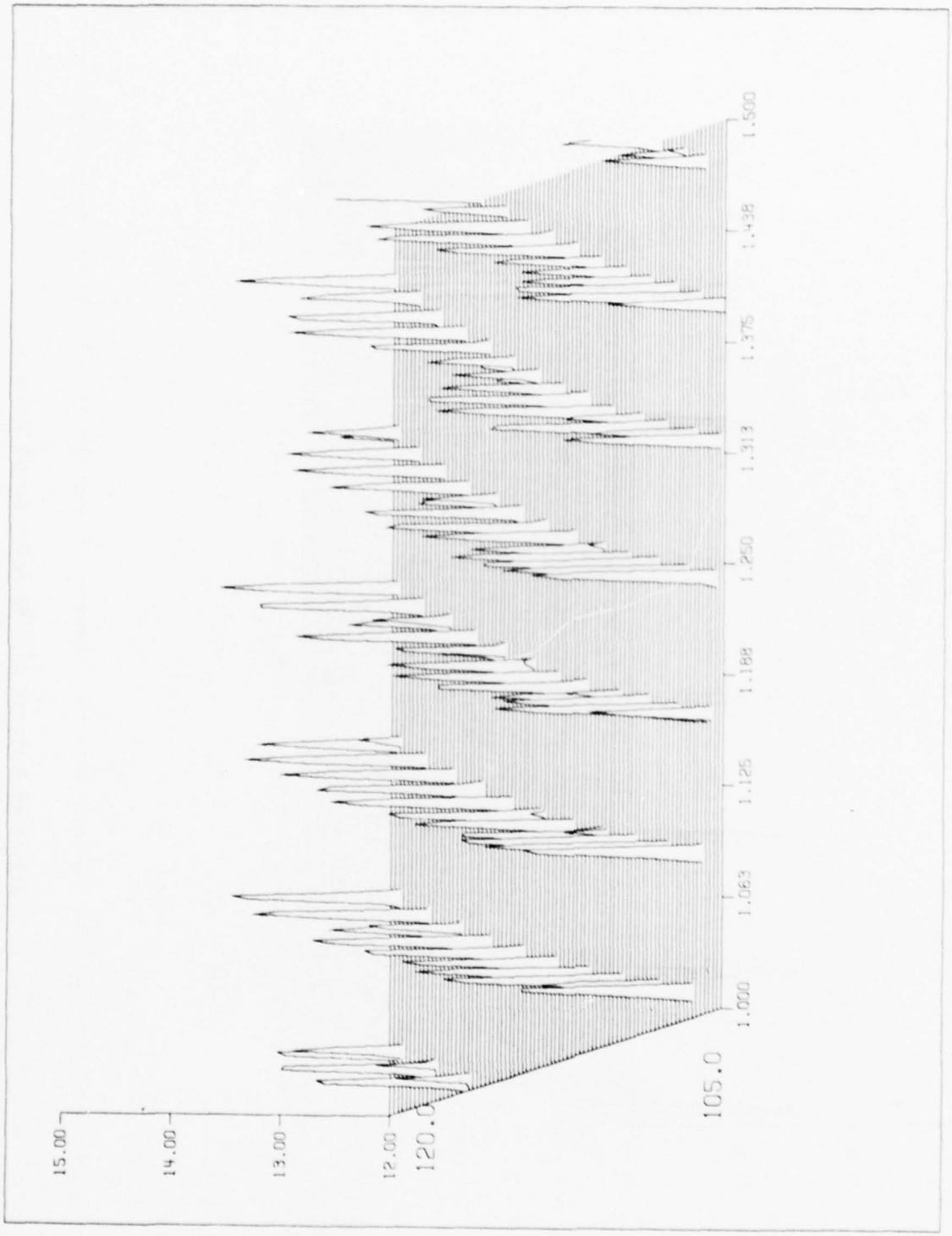

Figure 8h Response of five point target (cont.).

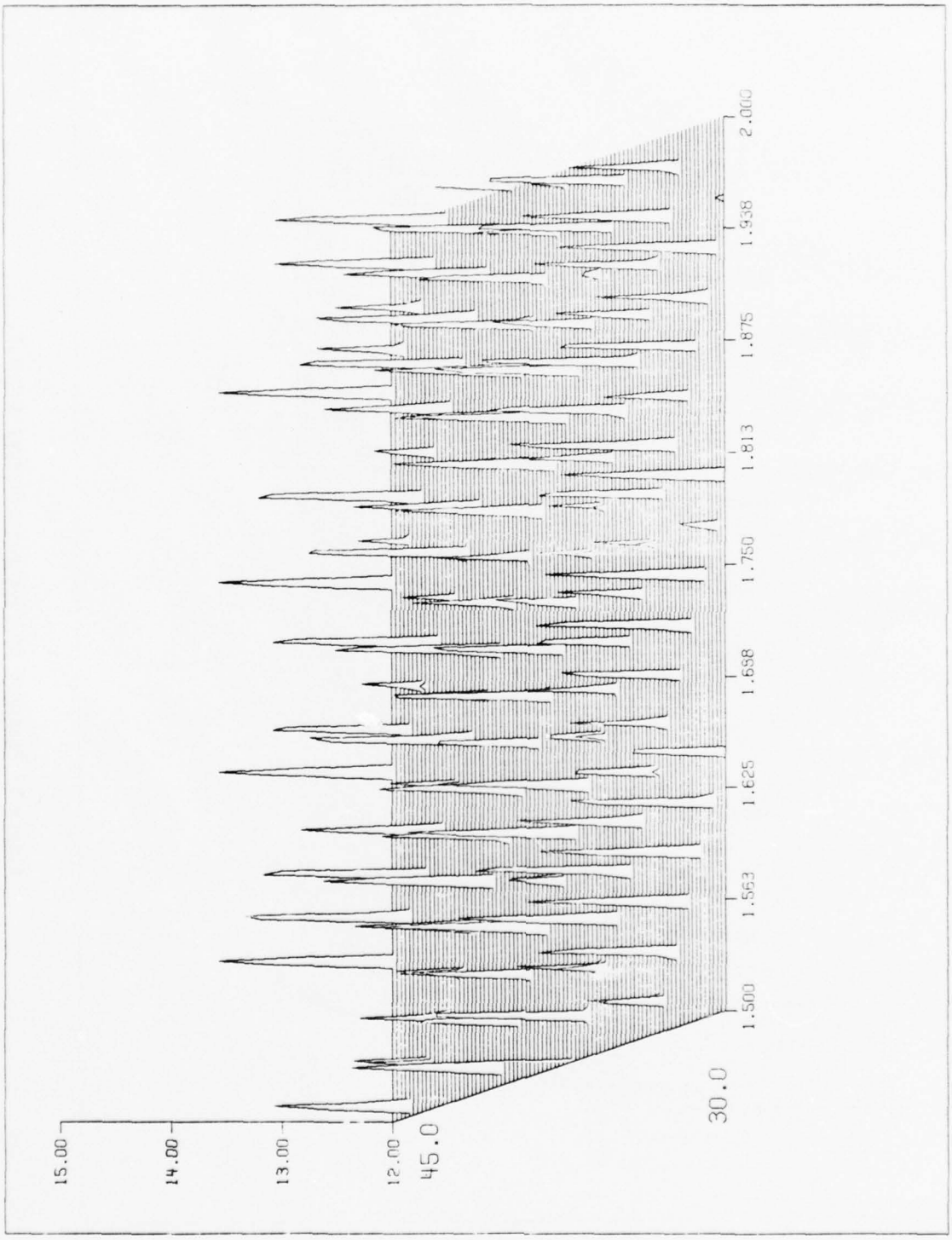

Figure 8i Response of five point target (cont.).

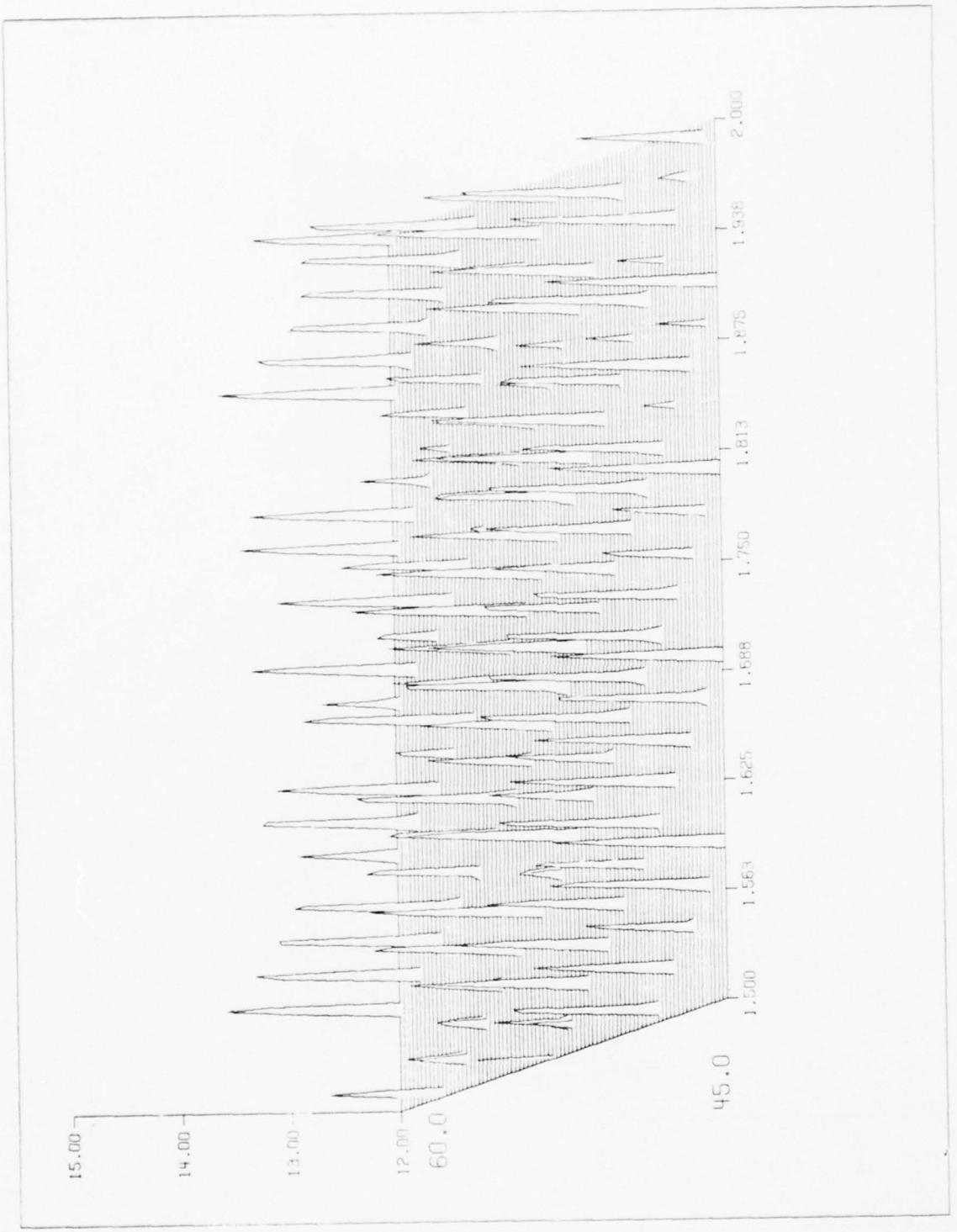

Figure 8j Response of five point target (cont.).

Figure 8j Response of five point target (cont.).

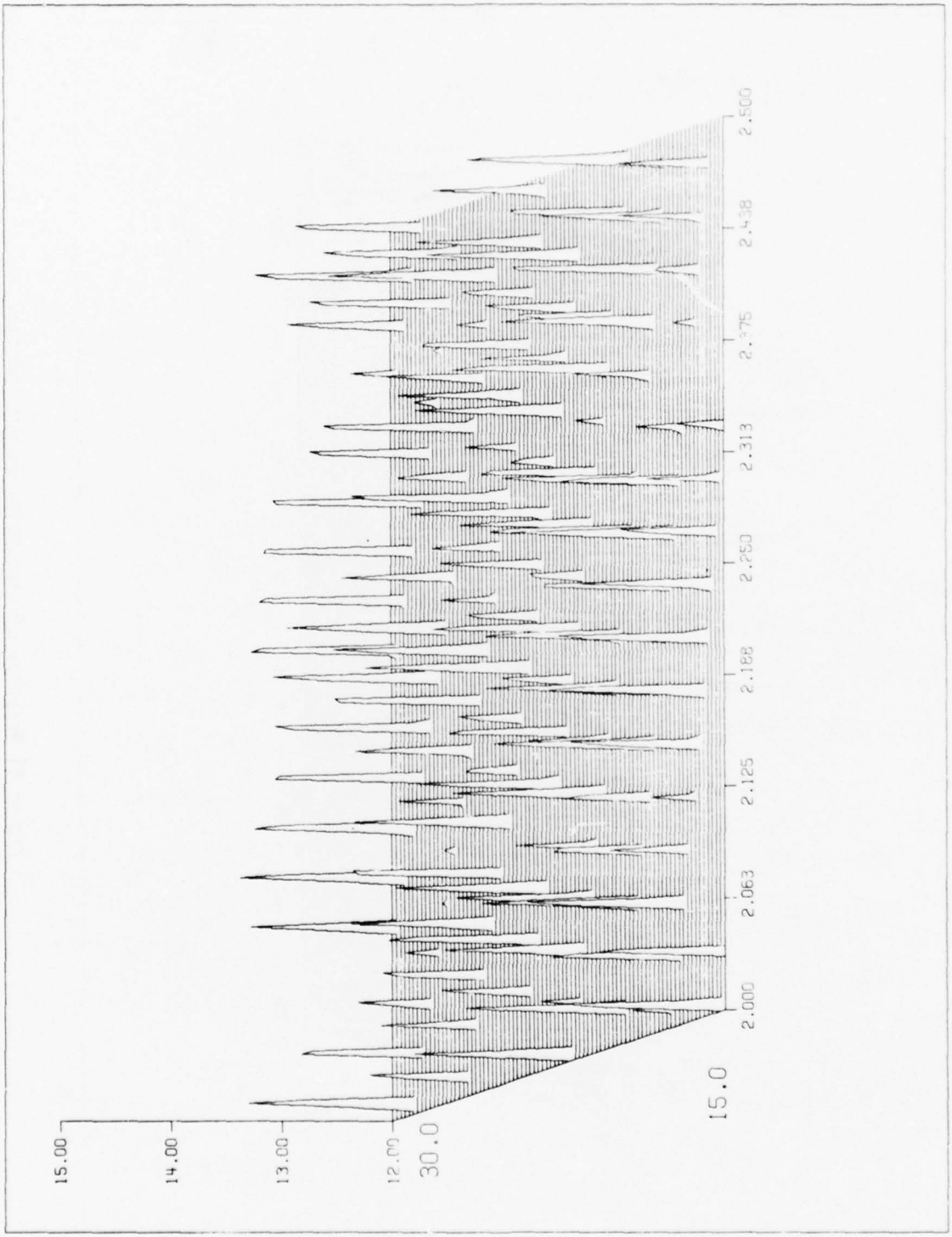

Figure 8k Response of five point target (cont.).

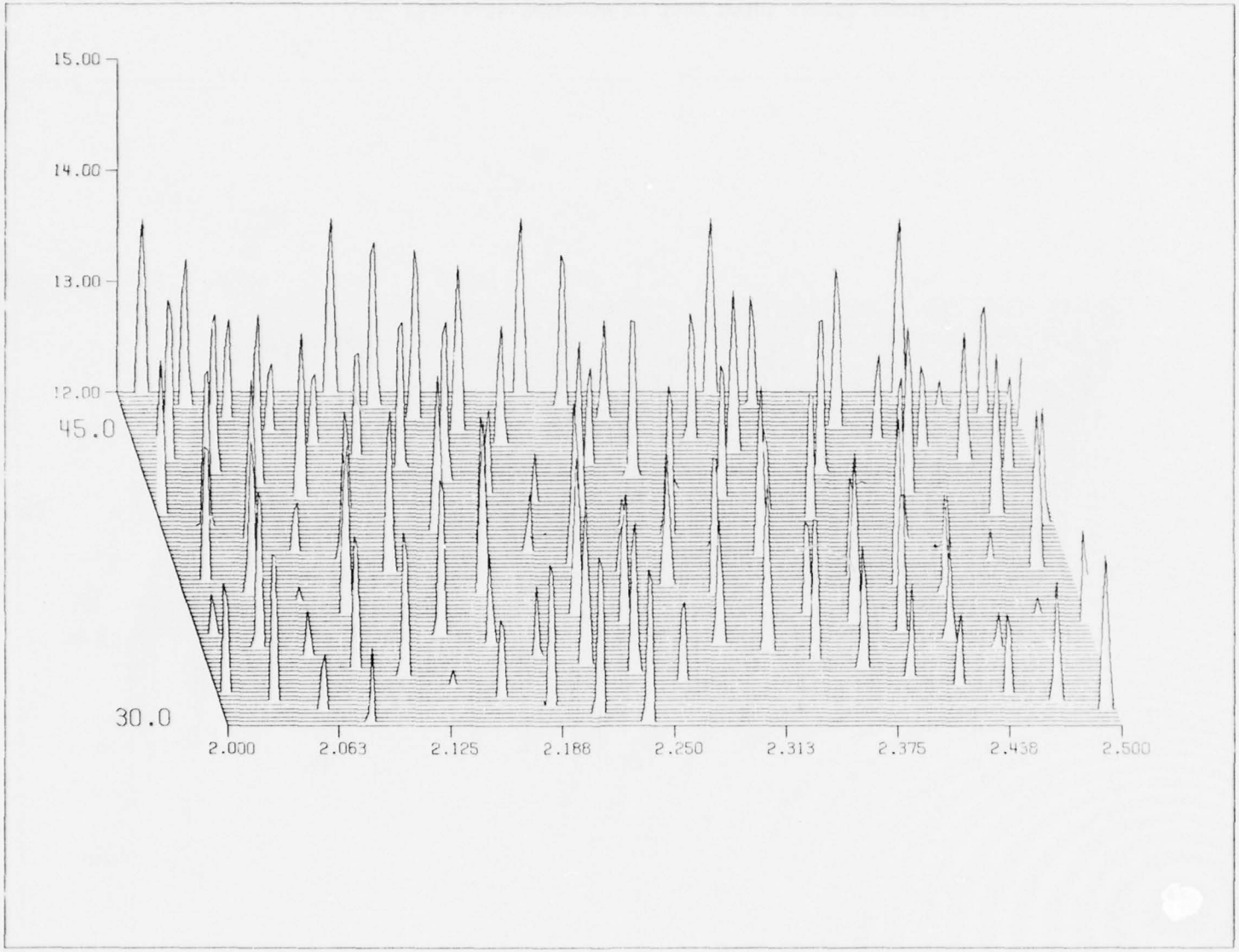

Figure 8l Response of five point target (cont.).

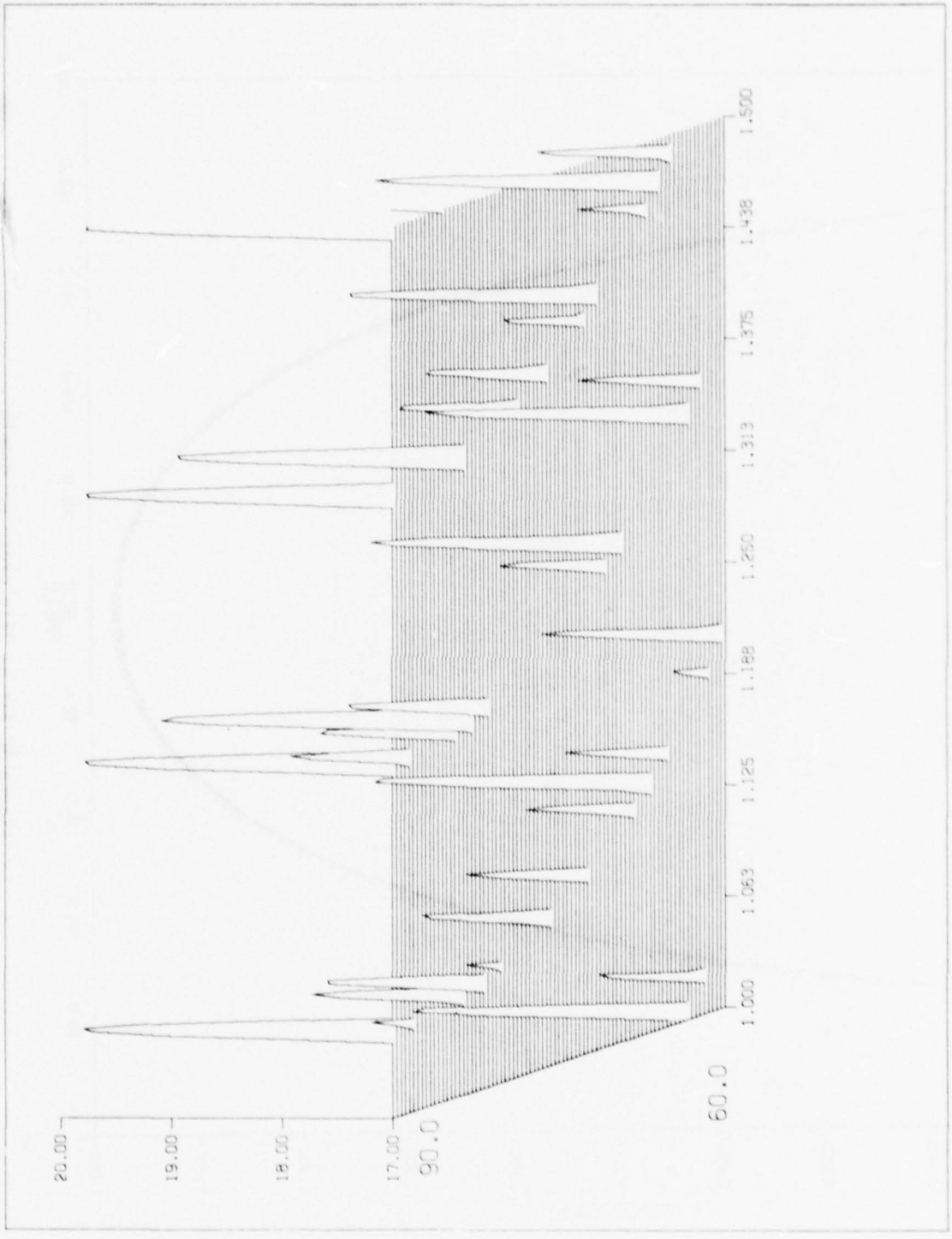

Figure 9 Response of ten point target.

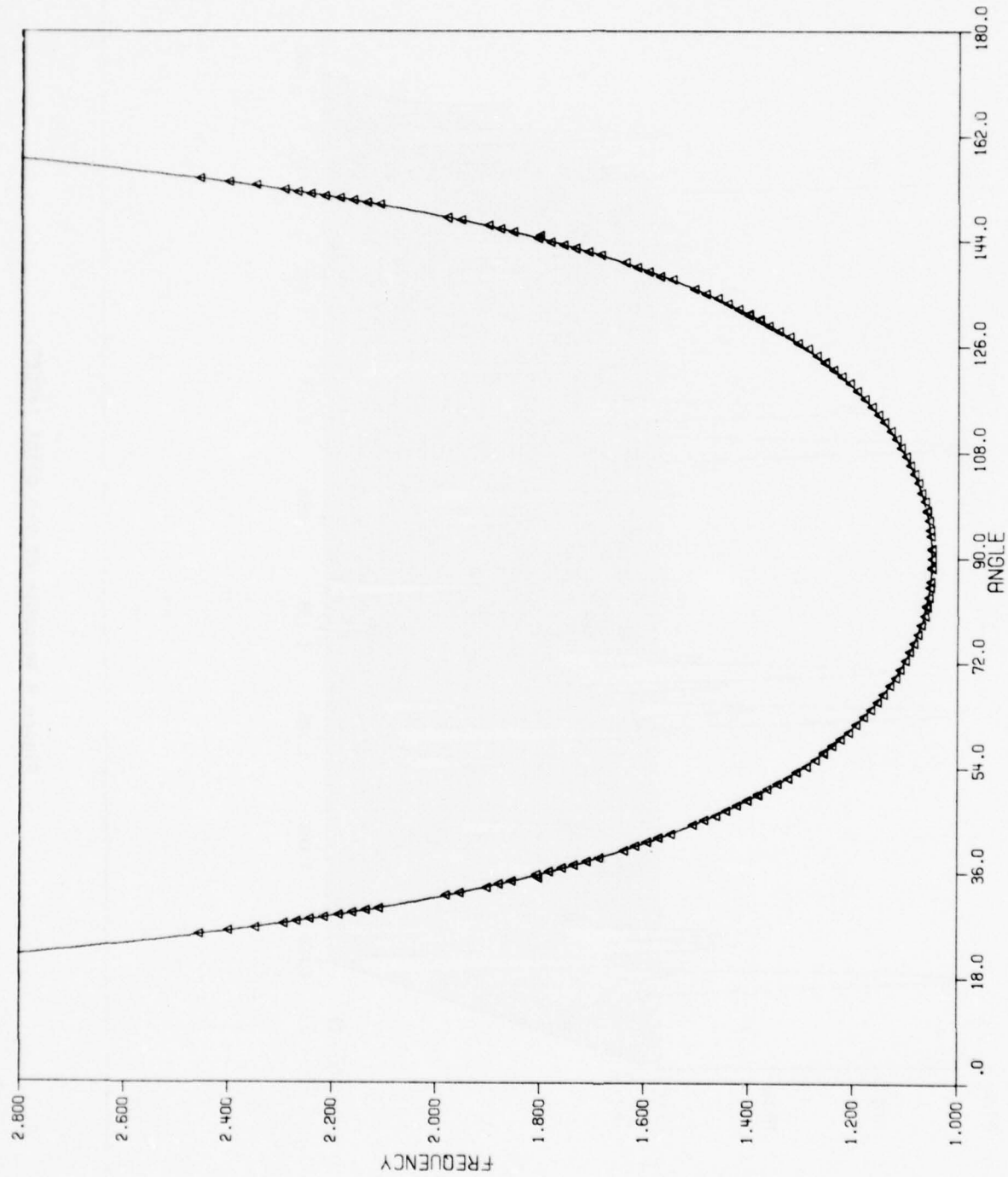

Figure 10 Fit of 16th order polynomial.

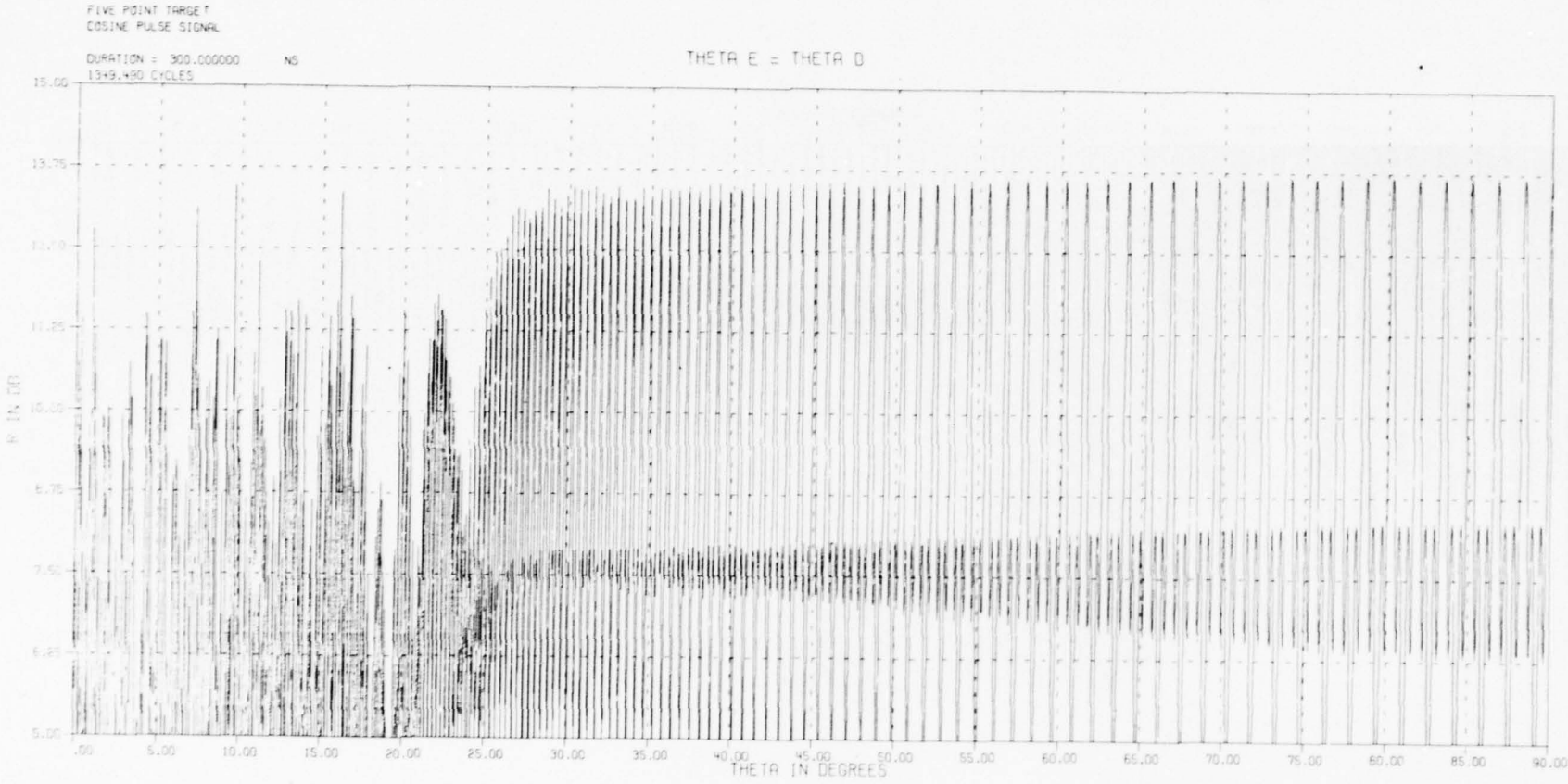

Figure 11 Response of target along curve of 16th order polynomial.

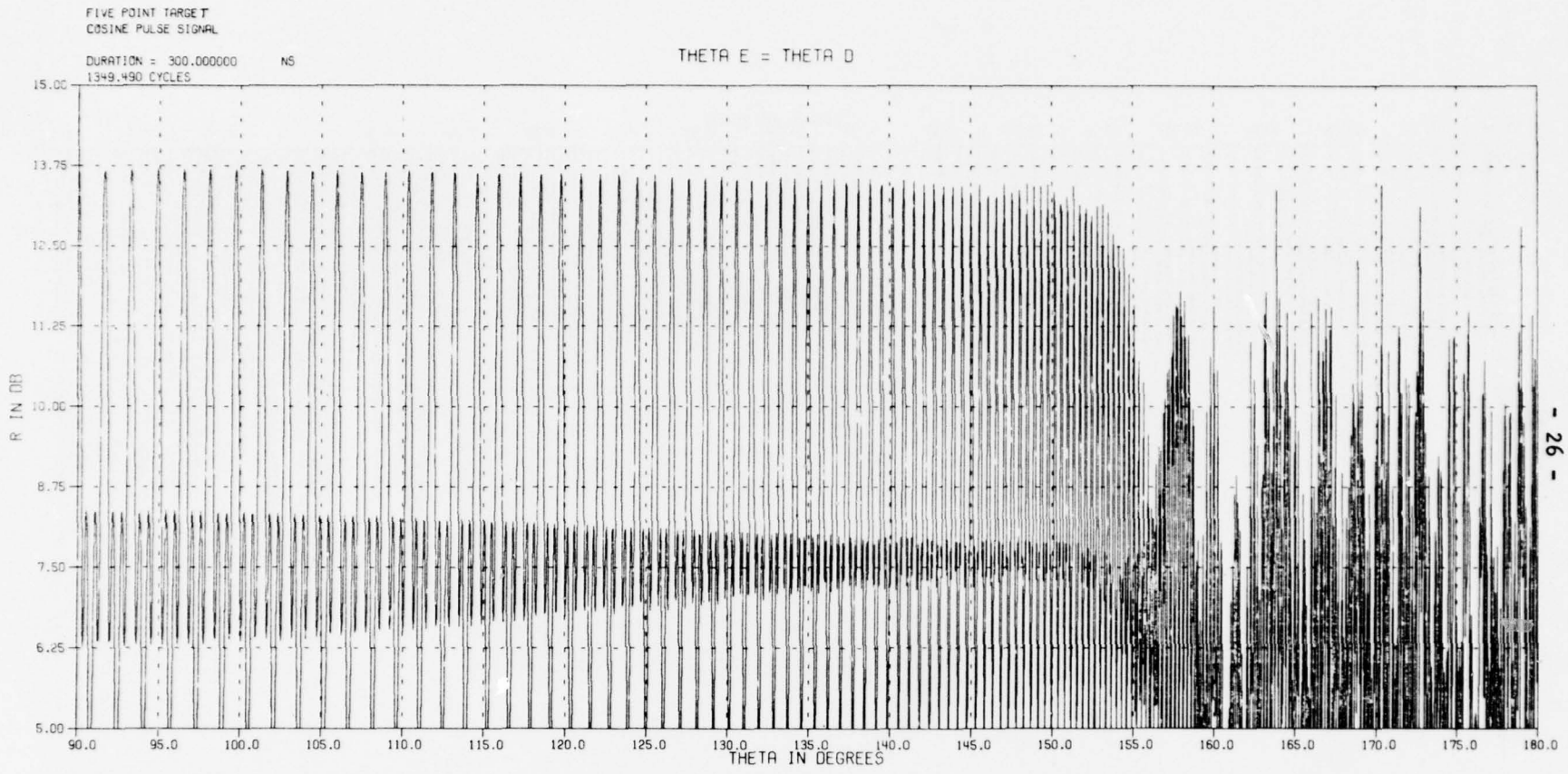

Figure 12 Response of target along curve of 16th order polynomial (cont.).

radar would track the target.

Table 1 Coefficients for 15th order polynomial, for first data set.

```
CF( 1) =   1.0493753E+00
CF( 2) =  -8.9428955E-18
CF( 3) =   1.6093651E-04
CF( 4) =   8.4572425E-20
CF( 5) =   1.4897936E-08
CF( 6) =  -2.3241124E-22
CF( 7) =   1.0072181E-11
CF( 8) =   2.8044422E-25
CF( 9) =  -3.8445882E-15
CF(10) =  -1.7257673E-28
CF(11) =   9.3811860E-19
CF(12) =   5.6498012E-32
CF(13) =  -3.6857554E-23
CF(14) =  -9.3640872E-36
CF(15) =  -4.5431032E-27
CF(16) =   6.1772326E-40
*** APPROXIMATION ACCEPTABLE ***
    MAX ERROR =  2.2423E-02   AVE ERROR =  2.0687E-03
```

Observing that the higher order coefficients in the series are quite small compared to others, perhaps a second or third order polynomial would be sufficient to track the target. Table 2 shows the coefficients for the least squares fit with a second degree polynomial.

Table 2 Coefficients for 2nd order polynomial, for first data set.

```
CF( 1) =   9.8514683E-01
CF( 2) =   2.3154825E-16
CF( 3) =   2.8877466E-04
*** APPROXIMATION ACCEPTABLE ***
    MAX ERROR =  2.6048E-01   AVE ERROR =   6.6897E-02
```

The target response along this curve is shown in Figure 13. We see that the second order curve is not accurate enough to predict the optimum frequency

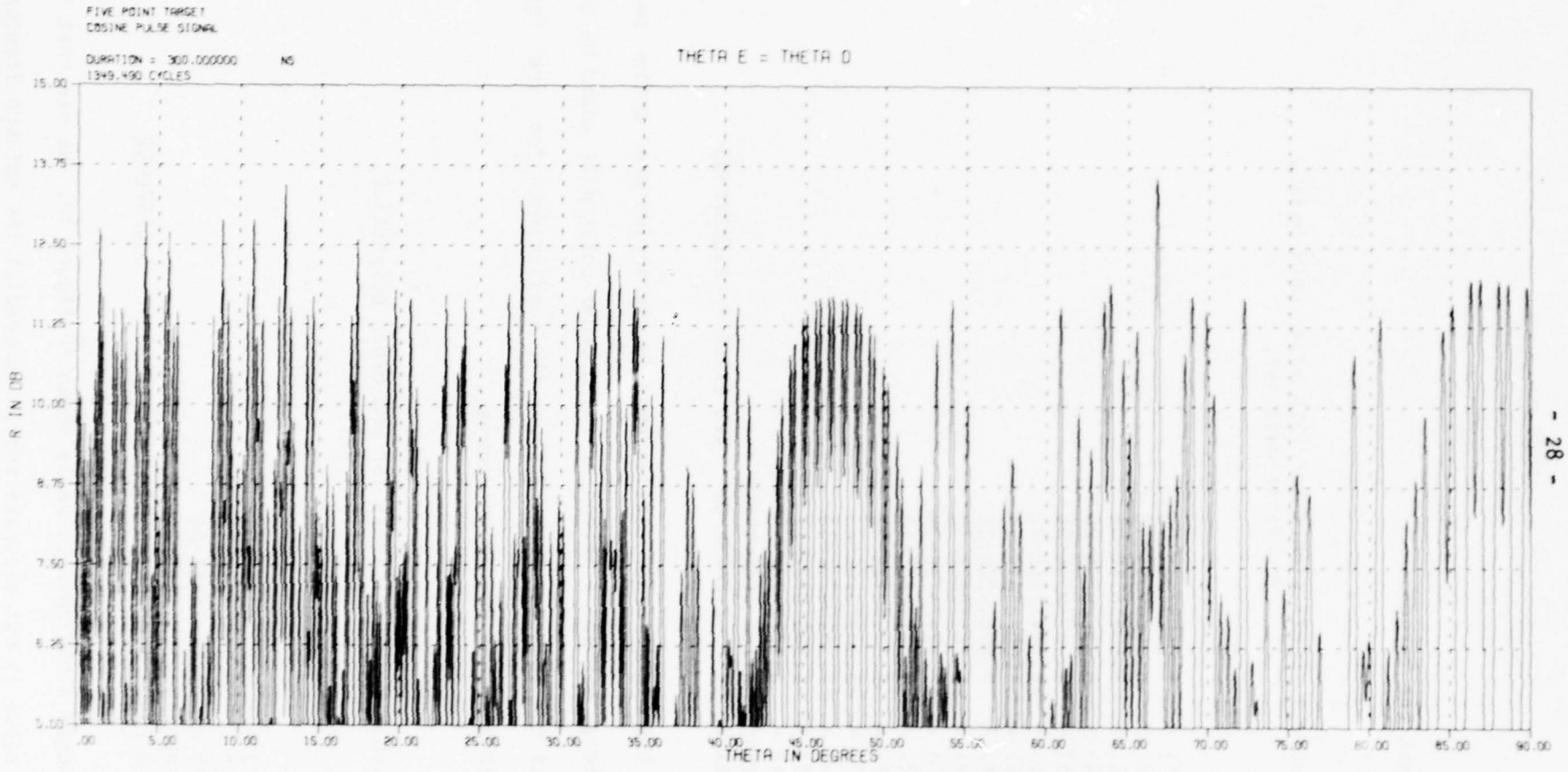

Figure 13 Response of target along curve of 2nd order polynomial.

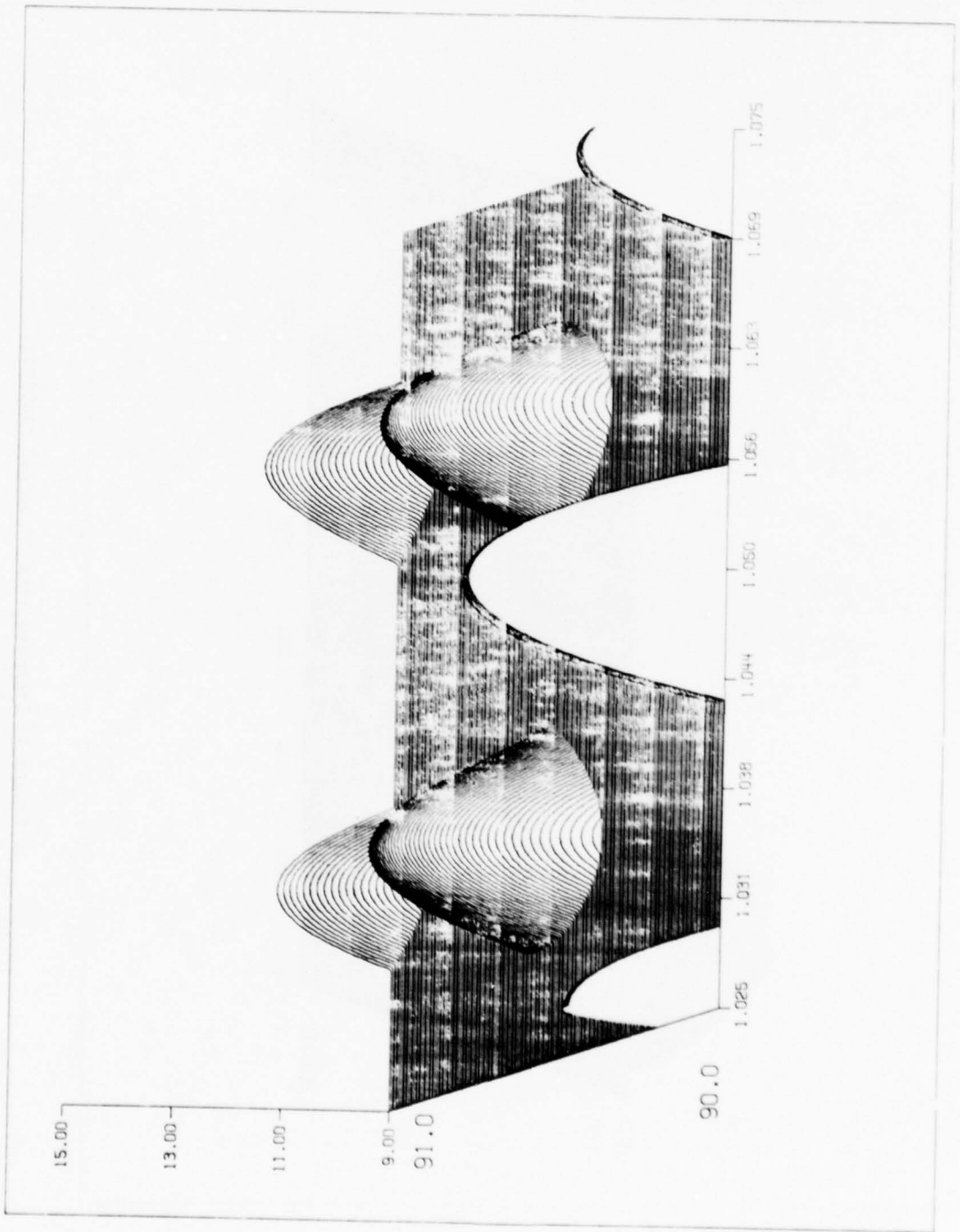

Figure 14 Expanded view of target response.

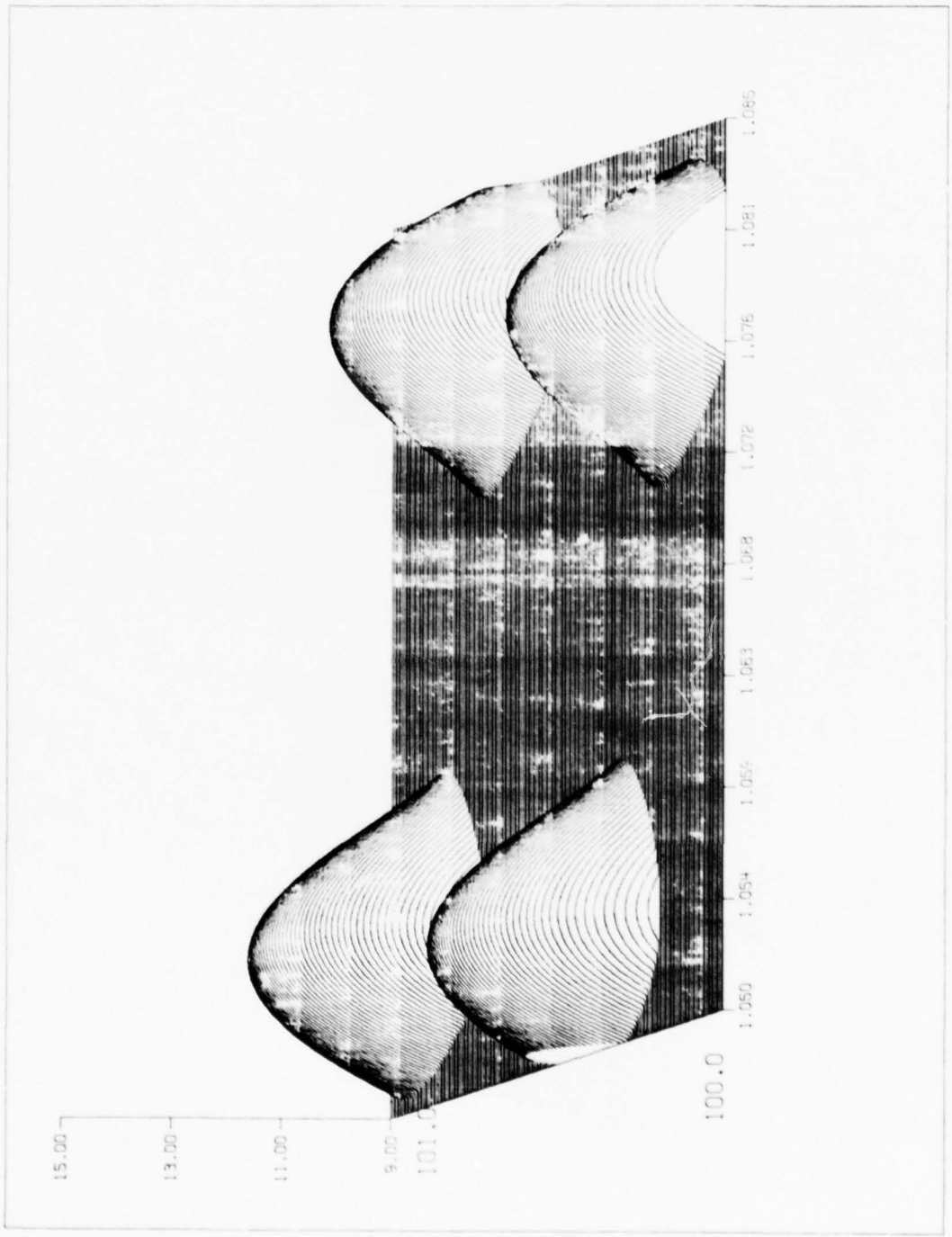

Figure 15 Expanded view of target response.

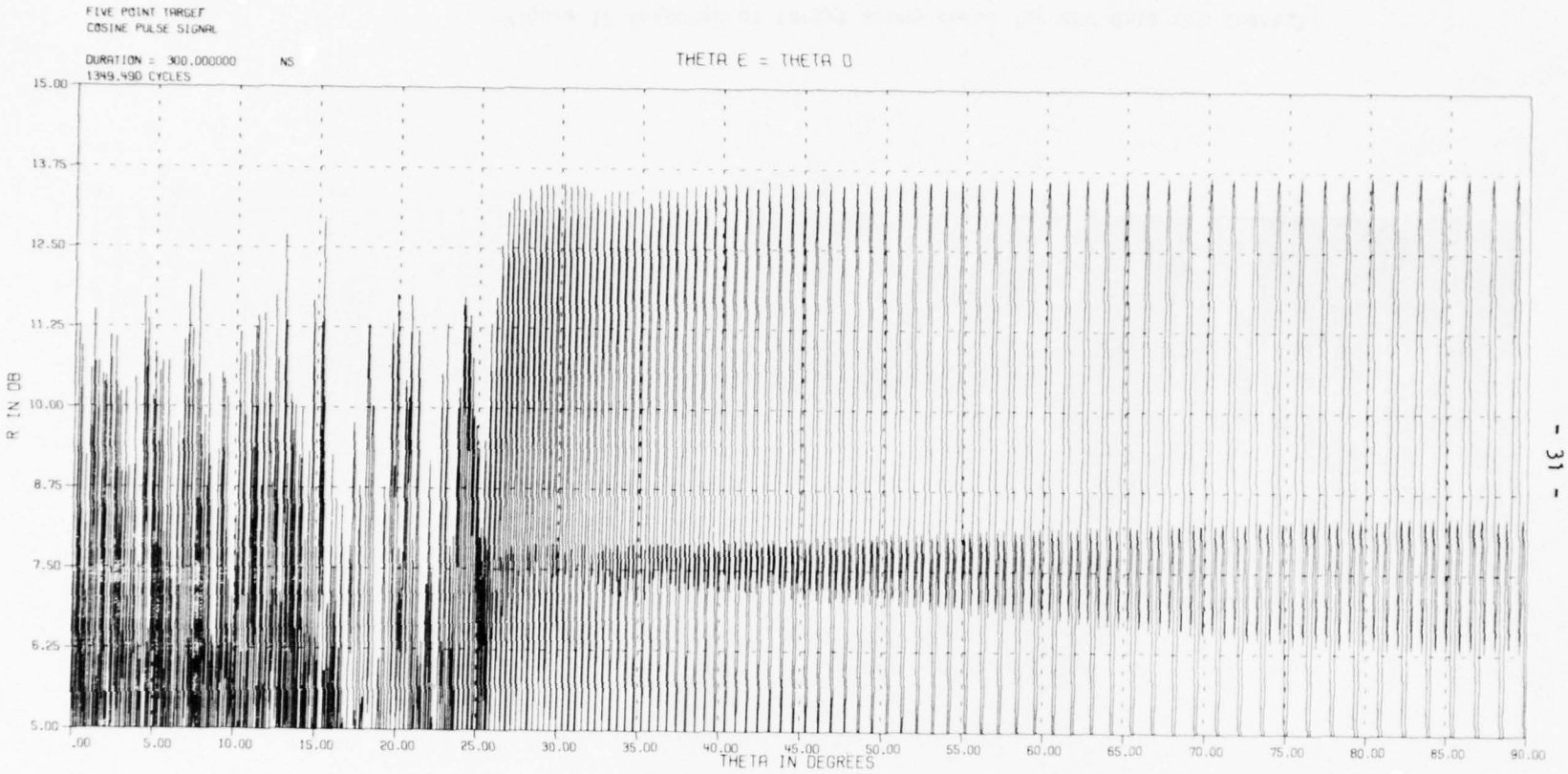

Figure 16 Response of target along curve for 2nd data set.

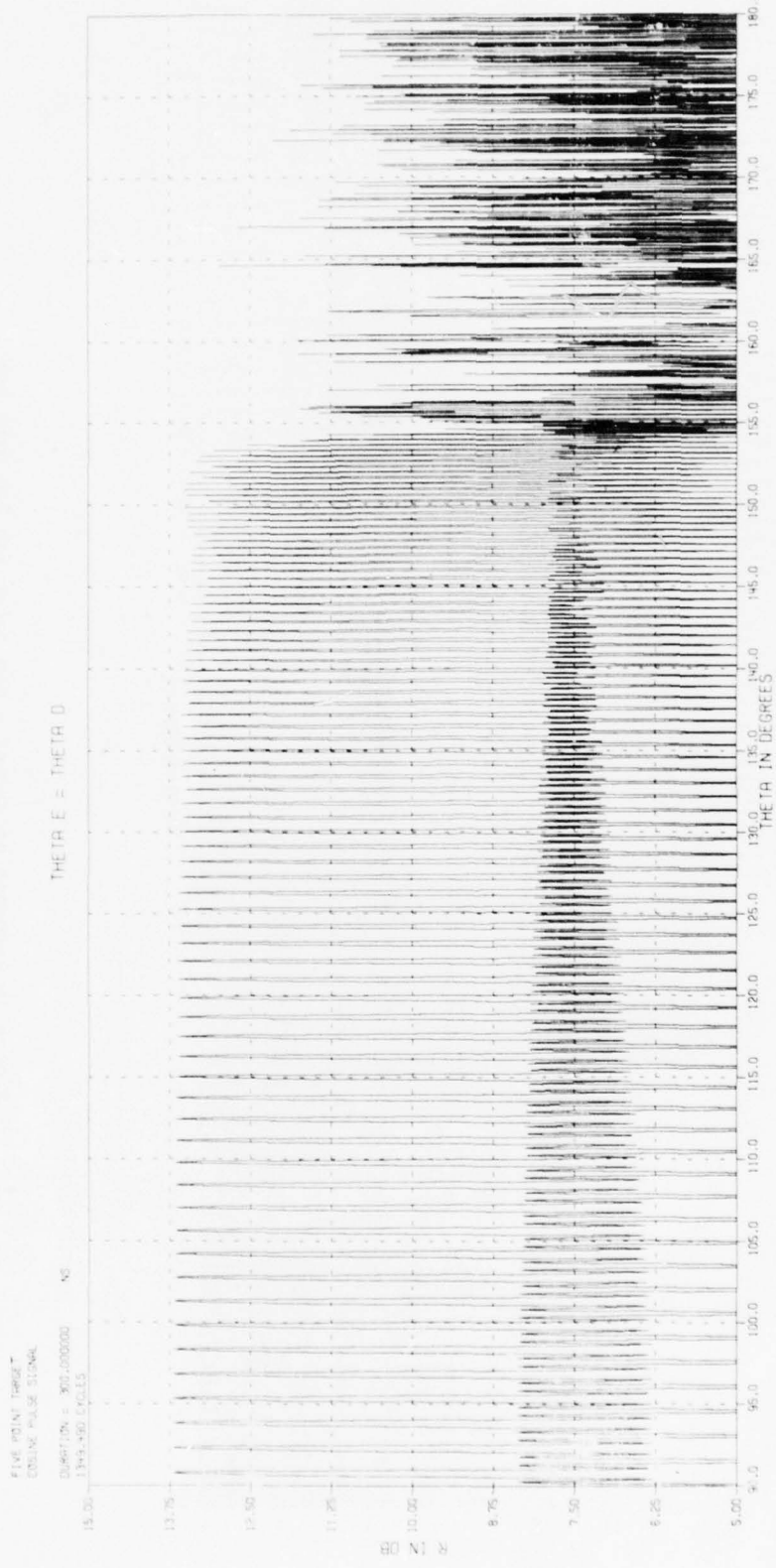

Figure 17 Response of target along curve for 2nd data set (cont.).

given the angle of incidence. Figures 14 and 15 show detailed views of the response along the curve of this first data set. It is seen that the peaks are separated by large valleys in which the response is not great enough to be significant.

Data was taken for a second curve to see if there was just a shift in origin between the two curves. Table 3 shows the coefficients for this curve and it is seen that there is quite a variation in the coefficient values. This means that the curves aren't simply translations of a single curve, but actually have different shapes. Figures 16 and 17 show the response of the target along this second curve, with f_c = 1.124 GHz at θ = 90°. The target responses in both cases are relatively periodic in the range of data points; however, outside of this range the response becomes very erratic due to the poor curve fit outside of the range of data.

Table 3 Coefficients for 15th order polynomial, 2nd data set.

```
BEST APPROX COEFS OF POWERS OF X
CF( 1) =   1.1241868E+00
CF( 2) =  -2.6812787E-18
CF( 3) =   1.6621612E-04
CF( 4) =   2.6045791E-20
CF( 5) =   4.3842827E-08
CF( 6) =  -7.2644725E-23
CF( 7) =  -3.5055444E-11
CF( 8) =   8.8491020E-26
CF( 9) =   3.1558381E-14
CF(10) =  -5.4969748E-29
CF(11) =  -1.3125499E-17
CF(12) =   1.8215026E-32
CF(13) =   2.7098962E-21
CF(14) =  -3.0685814E-36
CF(15) =  -2.1311769E-25
CF(16) =   2.0676587E-40
*** APPROXIMATION ACCEPTABLE ***
    MAX ERROR =  6.6921E-03   AVE ERROR =  1.4145E-03
```

4. NONSYMMETRICAL TARGETS

In the previous discussion, we were considering the response of symmetric targets, but it is likely that the target will appear to have no apparent symmetry when viewed by the radar. In such cases it is possible to generate symmetry in the target model by resolving the target into two components, each of which is symmetric about an axis, and when combined yield the original target.

For instance, if we have the three point target as shown in Figure 4, it can be considered as being made up of two six point components. The symmetric component, shown in Figure 18, has 6 points each with a reflection coefficient of 0.5. The antisymmetric component, Figure 19, has three points of reflectivity 0.5 and has three points of reflectivity - 0.5. The combination of the two components yields the original three point target.

The response of the three point target, Figure 20, doesn't show any apparent symmetry, and appears to be quite complicated. The response of the symmetric component, Figure 21a,b shows the general parabolic type curve that we saw in the previous section. The response of the antisymmetric component, Figure 22a,b, also shows the same curved structure as the symmetric component; however, the curves are shifted into the valleys of the previous curves. When the two components are combined, the peaks from one fall into the valleys of the other, and we get the total curve of the Figure 20. It is not apparent that the response is simply the sum of the two responses, due to phase combination effects; however, it is clear from the plots that there is a relationship between the response of the two components and the original target's response. This suggests that the response of a complex target can be considered to be a combination of the responses of simpler targets which may have characteristics which would allow the optimum fre-

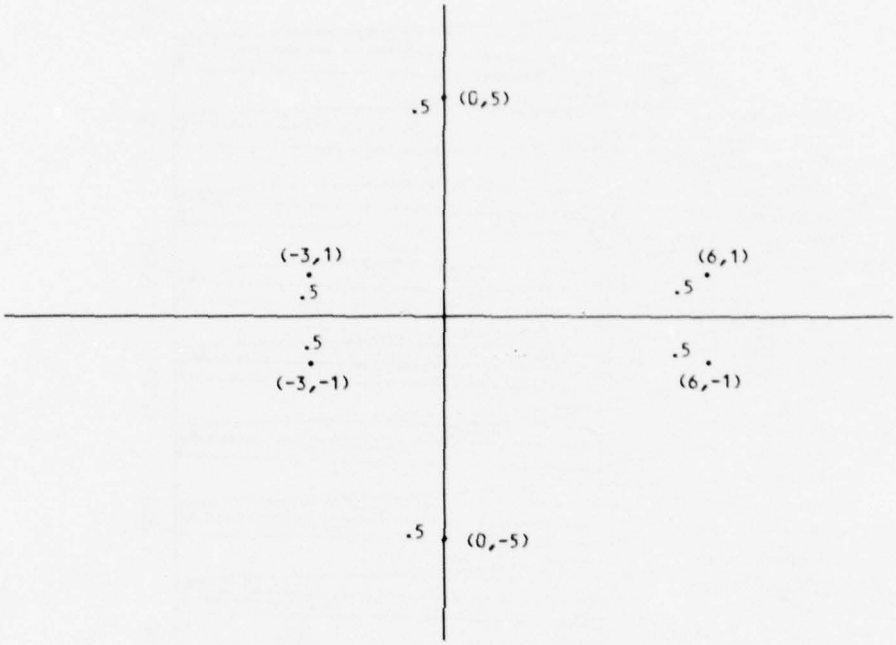

Figure 18 Symmetric Component of three point target.

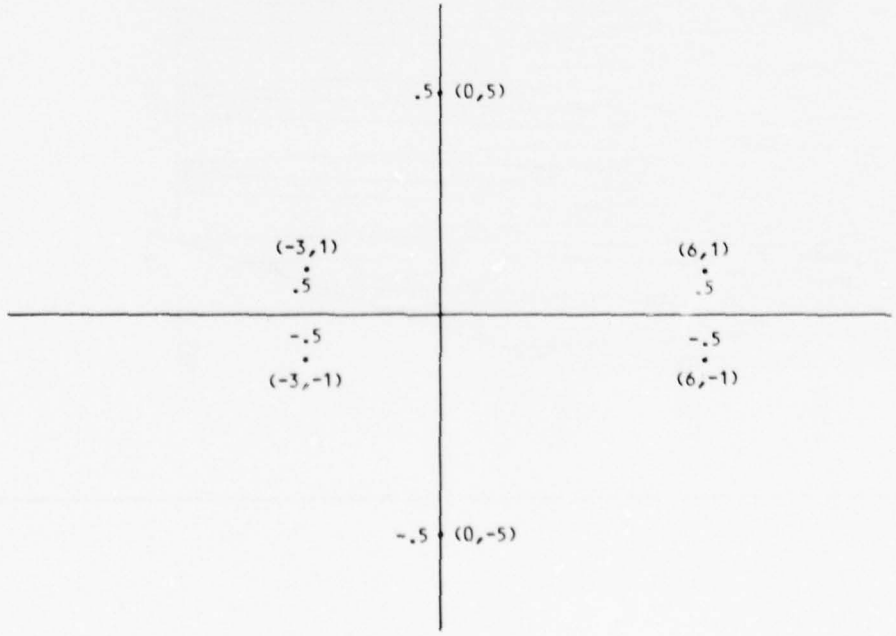

Figure 19 Anti-symmetric Component of three point target.

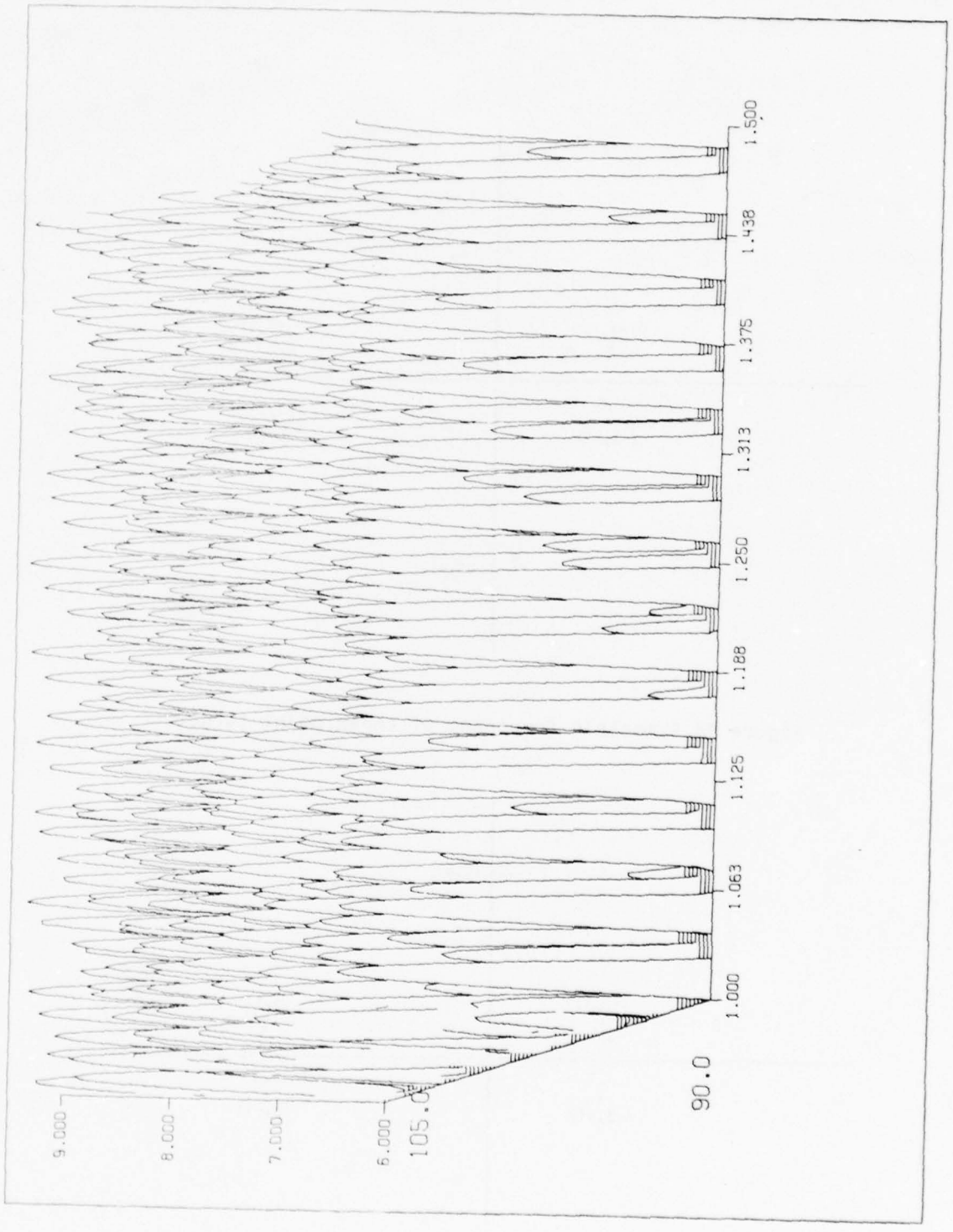

Figure 20 Response of three point target.

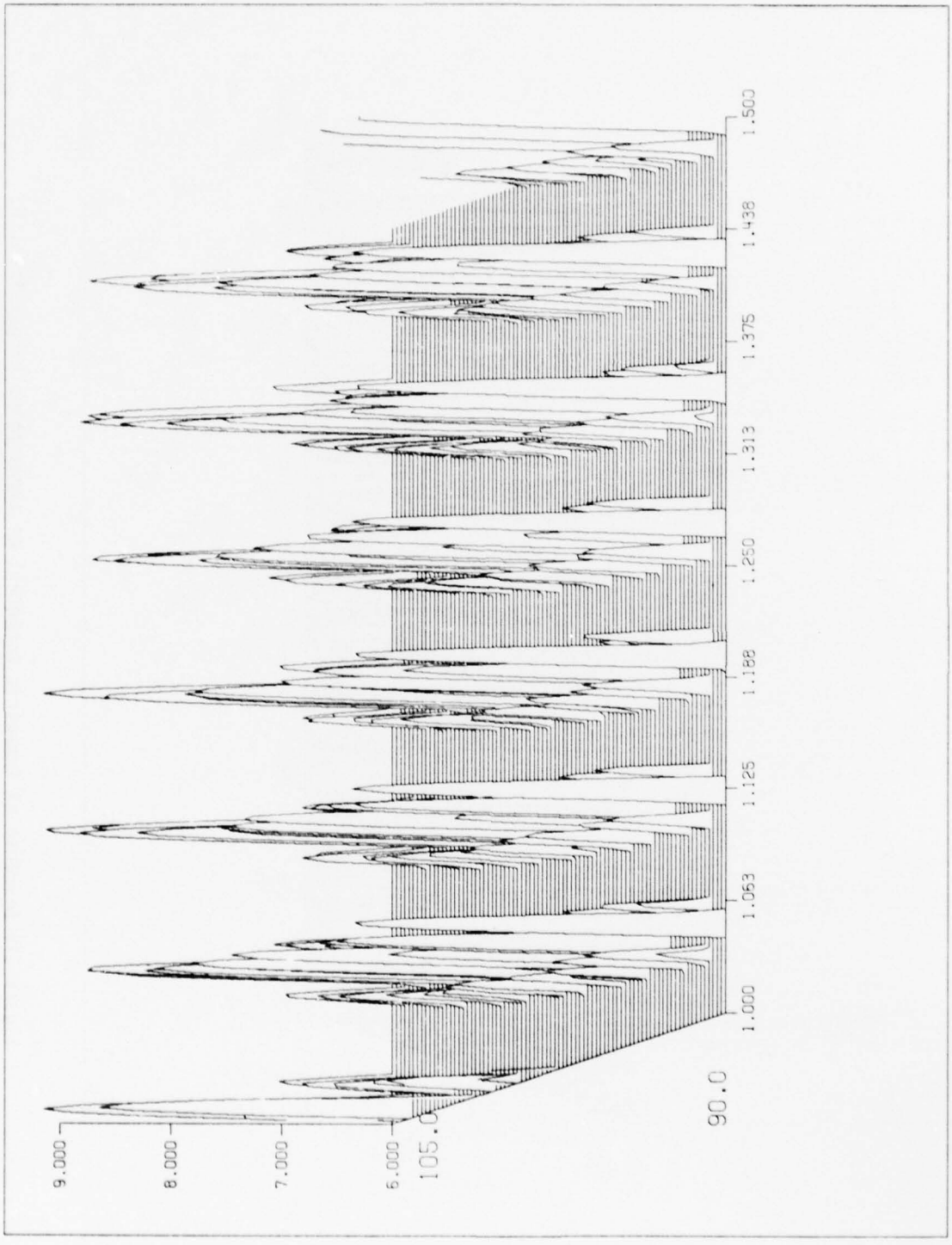

Figure 21a Response of Symmetric Component of three point target.

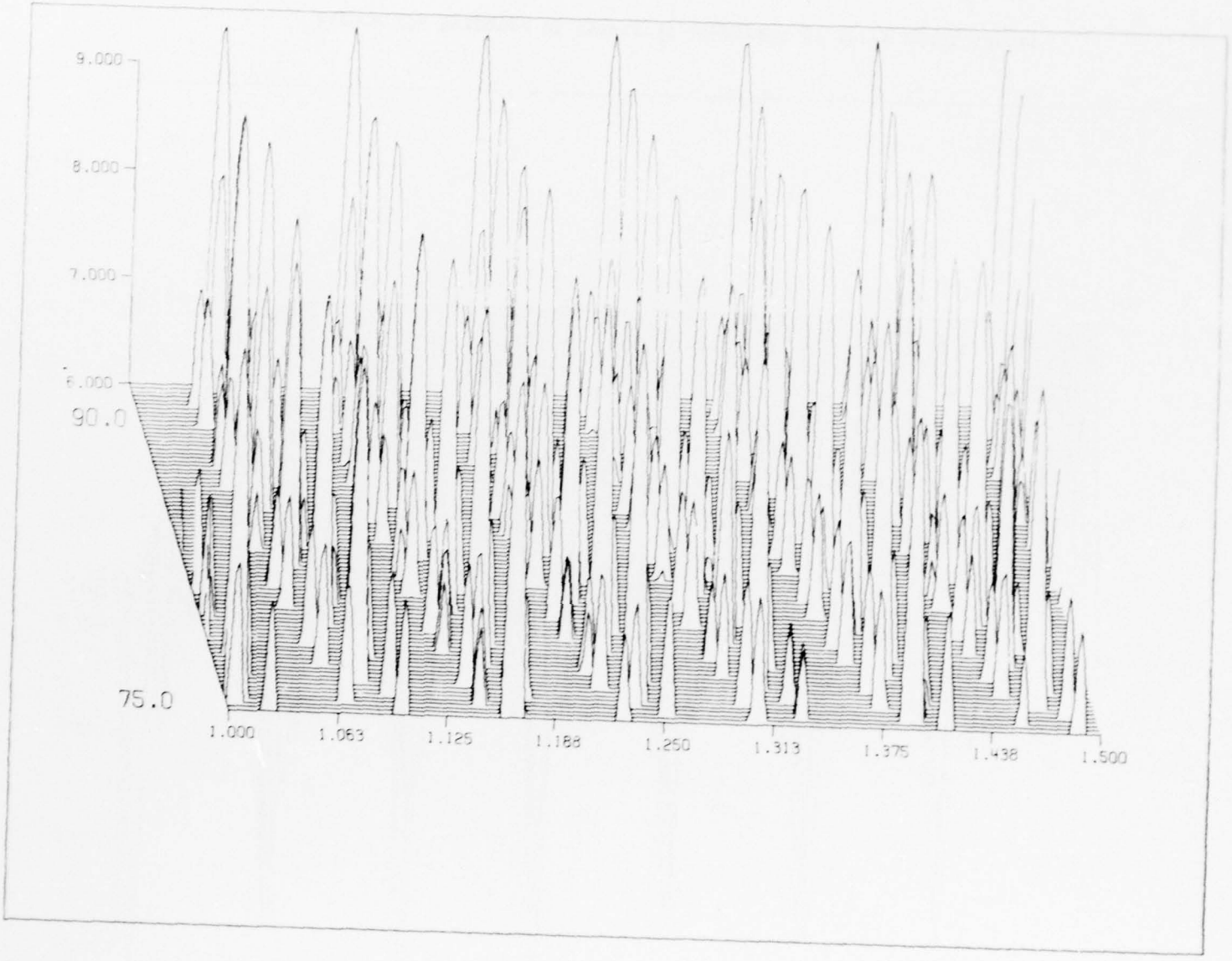

Figure 21b Response of Symmetric Component of three point target (cont.).

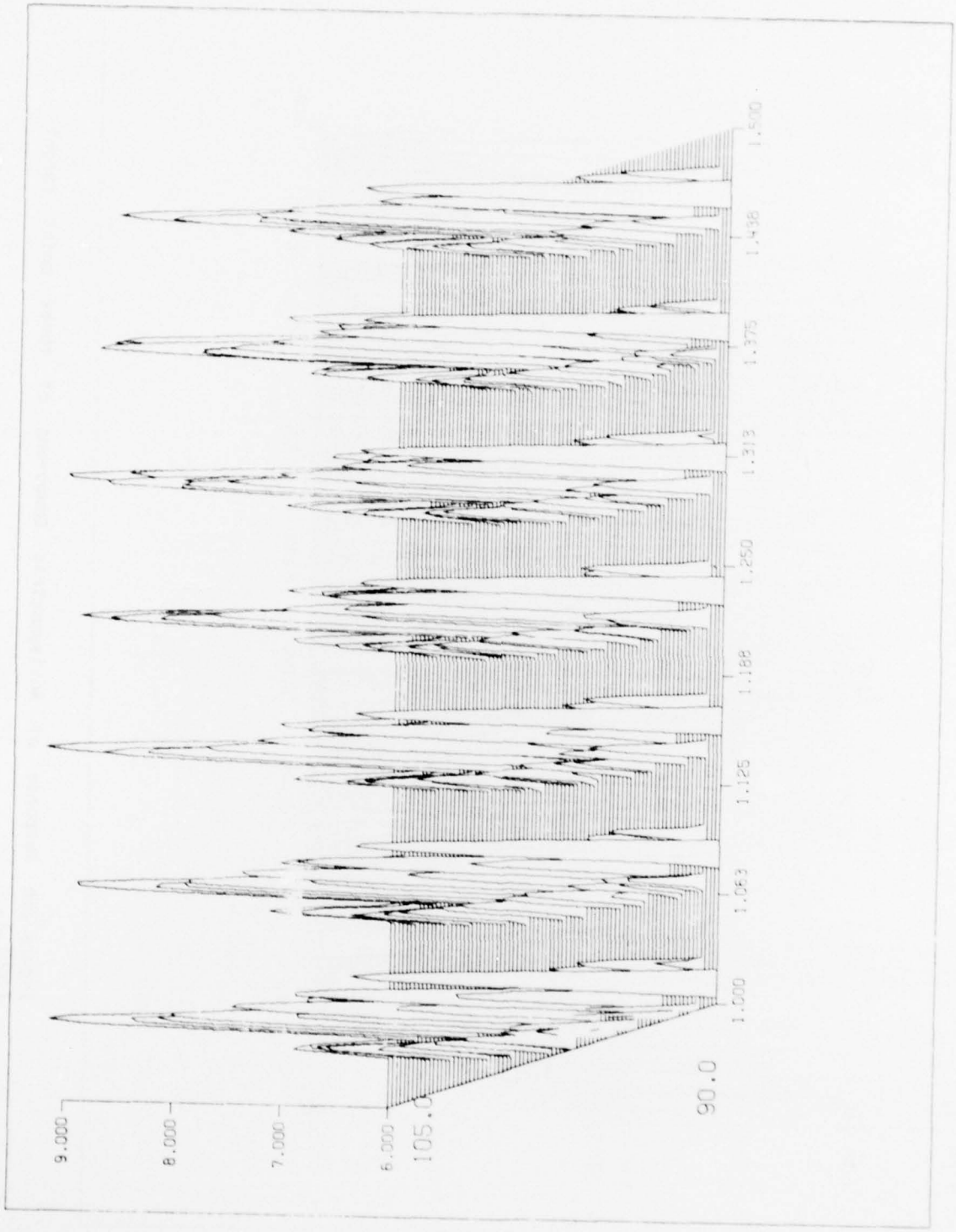

Figure 22a Response of Antisymmetric Component of three point target.

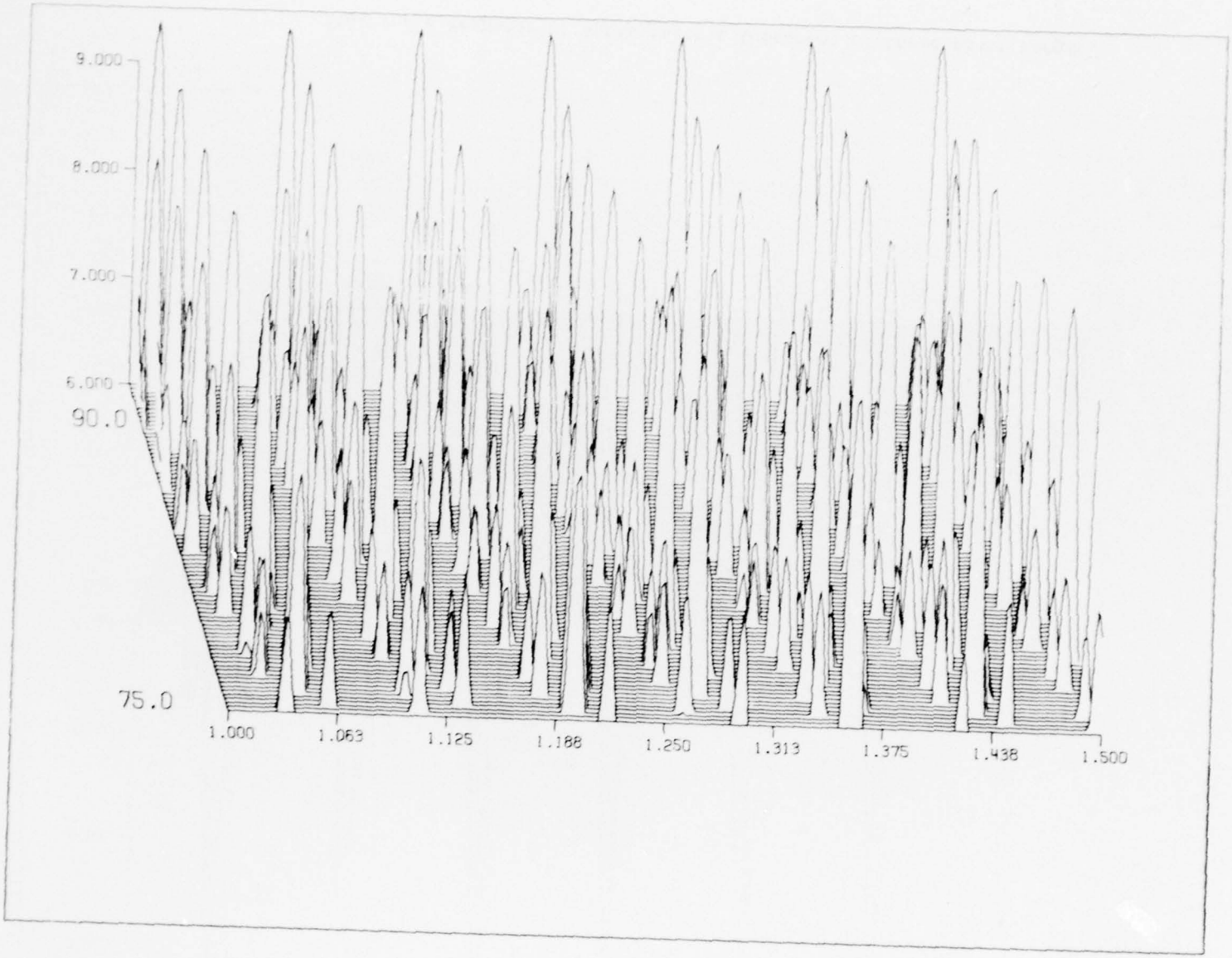

Figure 22b Response of Antisymmetric Component of three point target (cont.).

quency to be predicted given the incidence angle of the target.

We have examined target responses for a large number of cases as a function of angle and frequency; however, the relationship between the incident angle and time is not linear as a target flies by a radar installation. The functional form of this relationship depends upon the geometry of the flight path of the target relative to the radar. In the following the response of the radar system is shown as several different targets fly by the radar. The geometry of the system is shown in Figure 23. The target is assumed to be flying with a velocity of 1500 mph, and the radar has the target in view for 120 seconds. The angle of incidence ranges from 225^{o} to 315^{o}.

It is known from previous work that the five point target of Figure 2 shows a certain symmetry in its response, which could be utilized to predict a frequency providing a near optimum return, given the angle of incidence. The response of the target, as a function of time, when the carrier frequency is being predicted by the fifteenth order polynomial curve is shown in Figure 24. This is contrasted to the response of the target when the carrier frequency is fixed at f_c = 1.049375 GHz, a value which gives a maximum return at $\theta = 90^{o}$, and which is shown in Figure 25. Both curves achieve R_{max} = 13.704 dB at $\theta = 90^{o}$, which is .276 dB less than the theoretical maximum of 13.98 dB for the five point target. The difference between these two curves is that the fixed carrier signal only achieves this high value for 5 peaks, all near $\theta = 90^{o}$; whereas, when the carrier frequency is being varied according to the fifteenth order polynomial, the peaks occur every 1.7 seconds throughout the entire time that the target is in view of the radar. This is quite an improvement over the fixed frequency system, but requires that you generate the prediction curve for the target.

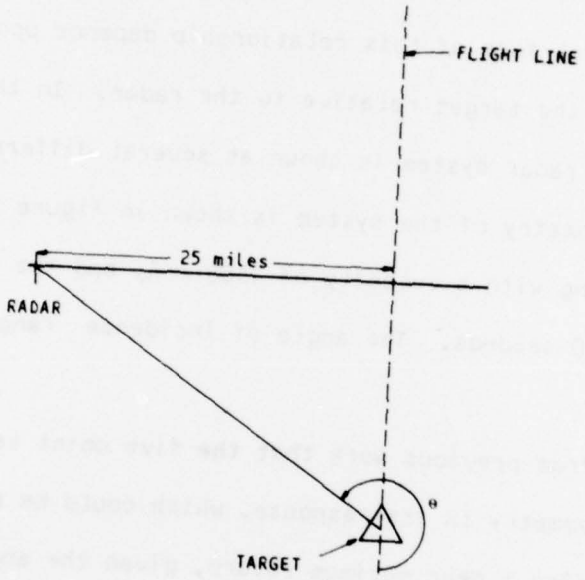

Figure 23 Radar System Geometry.

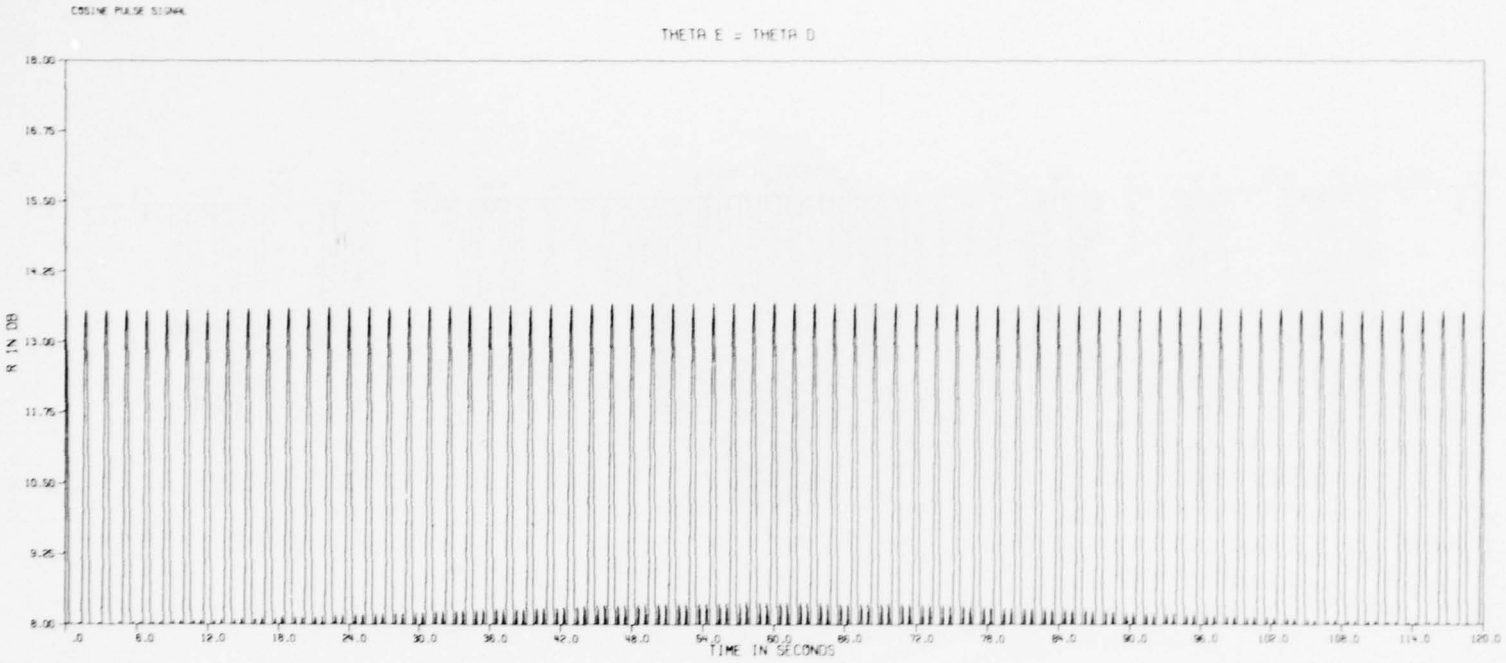

Figure 24 Response of five point target when carrier frequencies is predicted by 15th order polynomial.

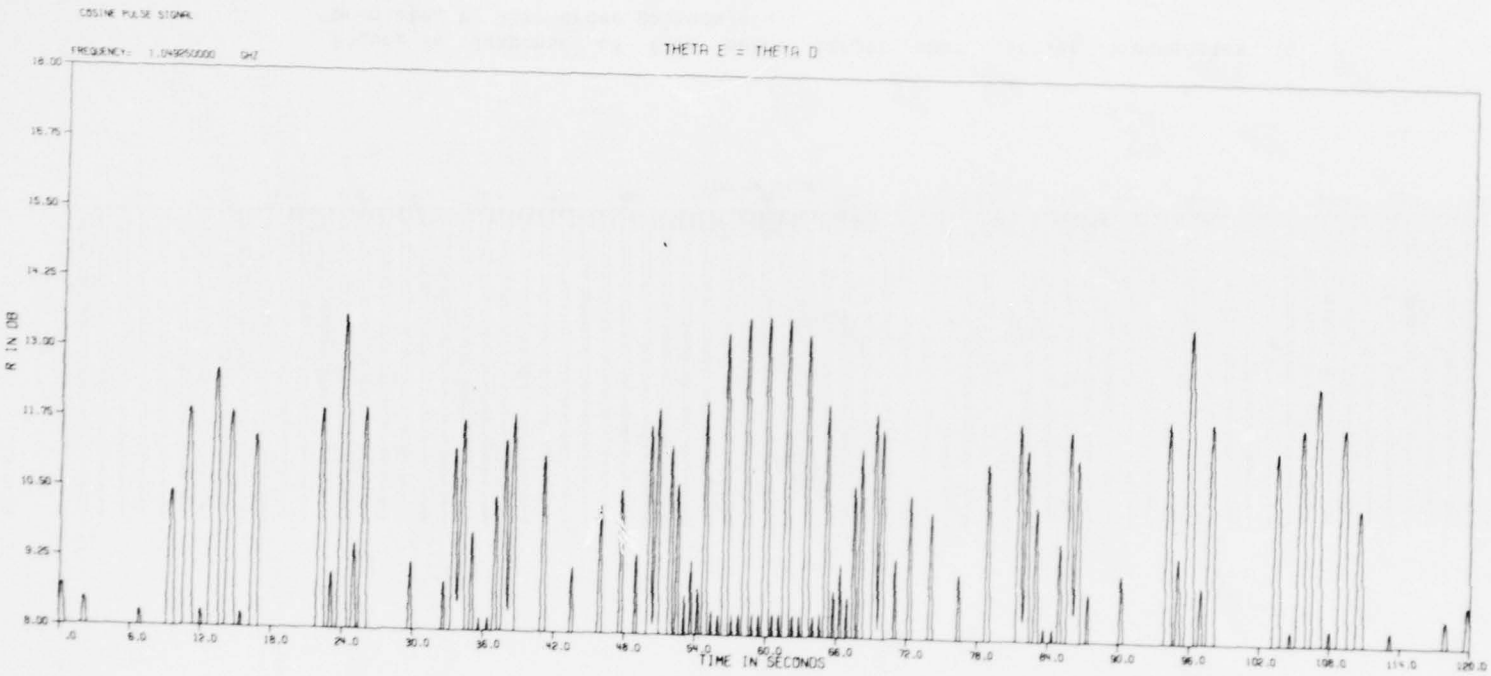

Figure 25 Response of five point target when carrier frequency is fixed.

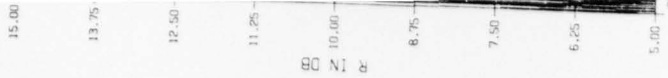

The response of the six point nonsymmetric target as a function of frequency, for $\theta = 90^{o}$ is shown in Figure 26. It is seen that the response takes on its maximum values at four frequencies in the range of frequencies presented. The response of the system is shown for the fixed frequency radar case, for each of these four frequencies, in Figures 27a-d. There doesn't appear to be any correlation between these returns and there isn't structure in the returns. Some technique of symmetry generation should be used to generate the required curves for this target.

5. SUMMARY

This work has shown the presence of spatial symmetries which may allow a radar system to predict a frequency which will give a near maximum response as the target approaches the radar. If the target is complex then the target may be resolved into simpler components, which have desirable characteristics, and symmetries that may be exploited when tracking the target. An efficient method for the approximate evaluation of the time ambiguity functions for complex pulse envelope shapes has also been presented.

6. REFERENCES

(1) Cooper, G. R. and C. D. McGillem, "Space-Time Signal Processing of Radar Returns," Phase Report, RADC-TR-78-89, April 1978, Phase II, ADA055758.

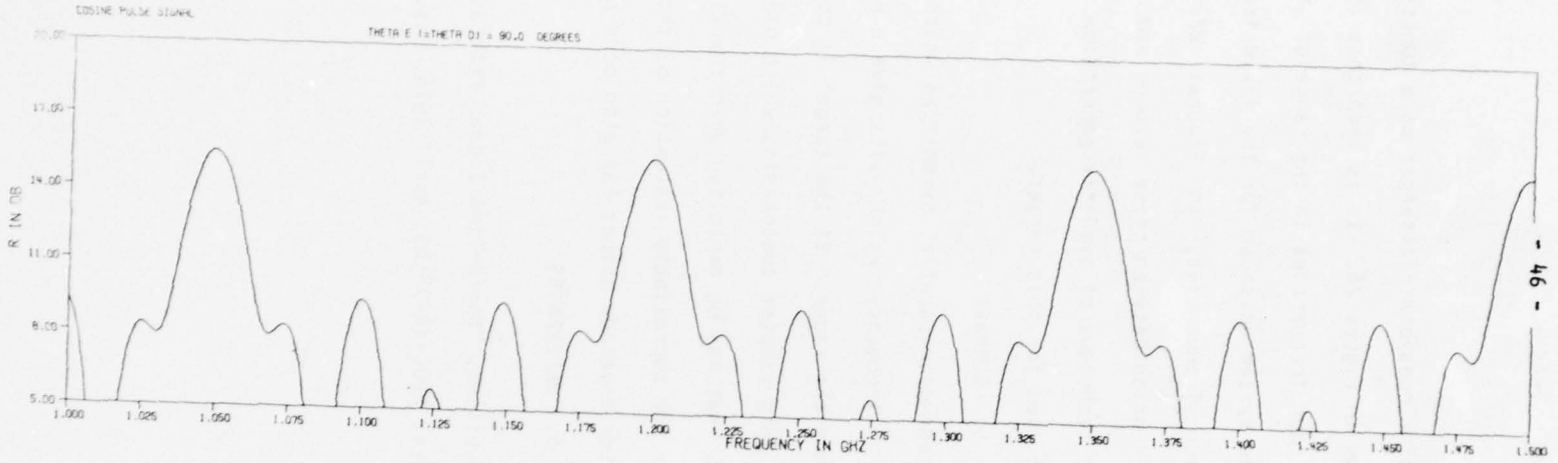

Figure 26 Response of six point target as a function of frequency.

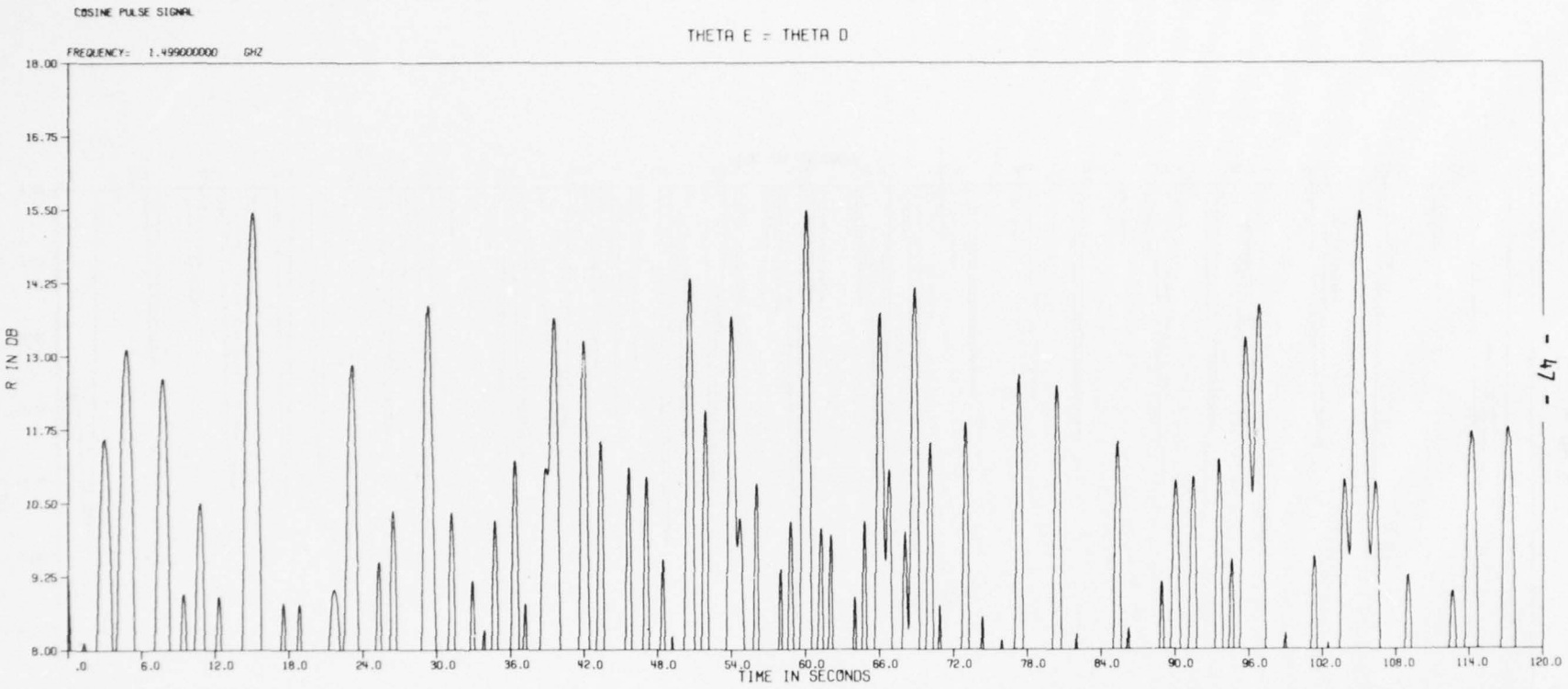

Figure 27a Response of six point target for fixed carrier frequency.

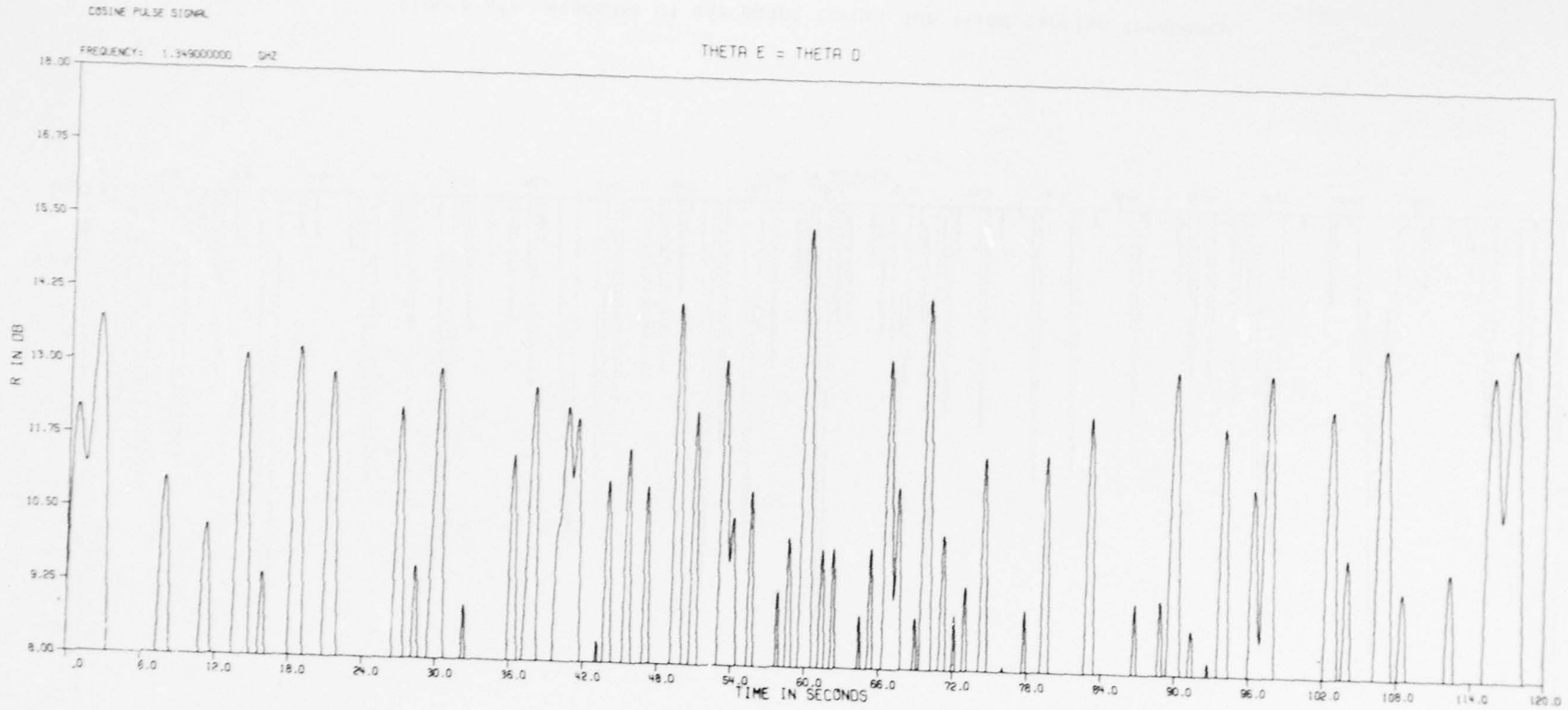

Figure 27b Response of six point target for fixed carrier frequency (cont.).

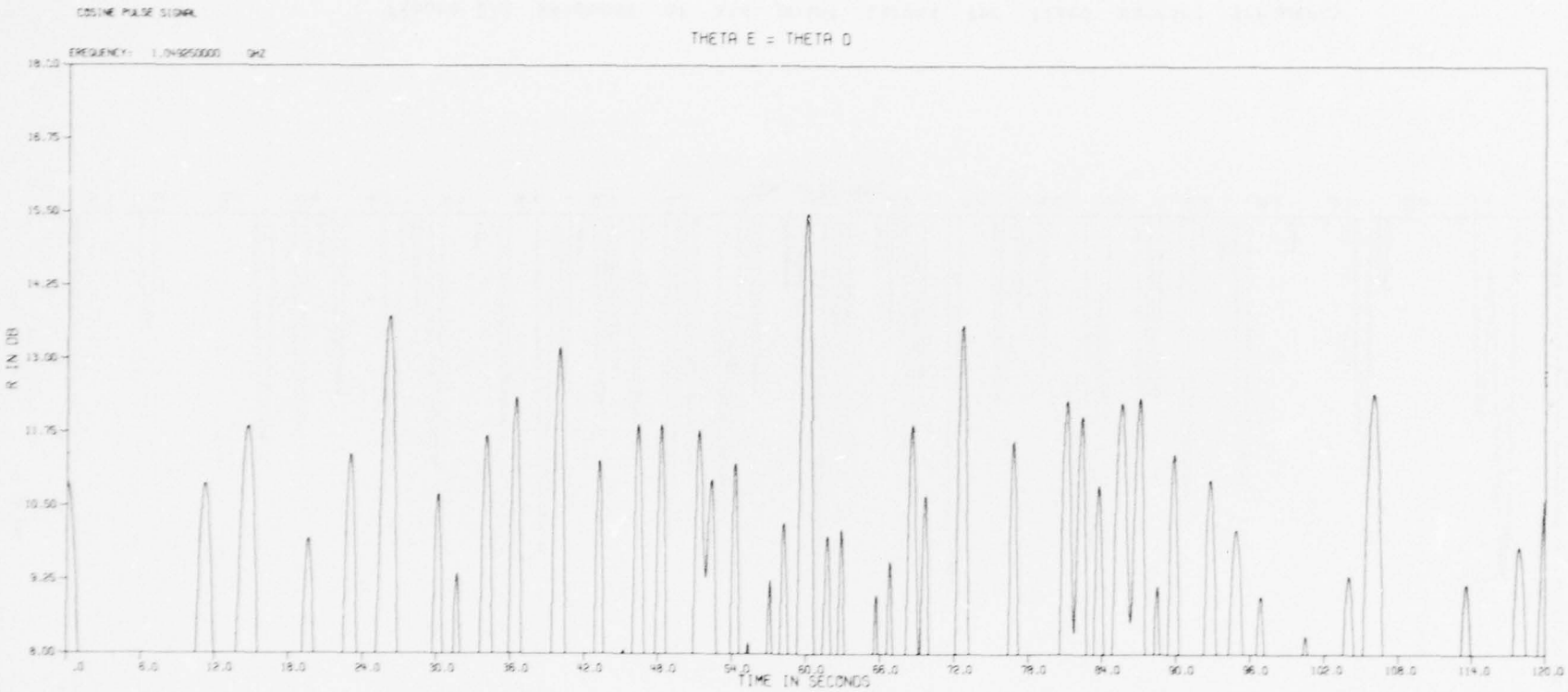

Figure 27c Response of six point target for fixed carrier frequency (cont.).

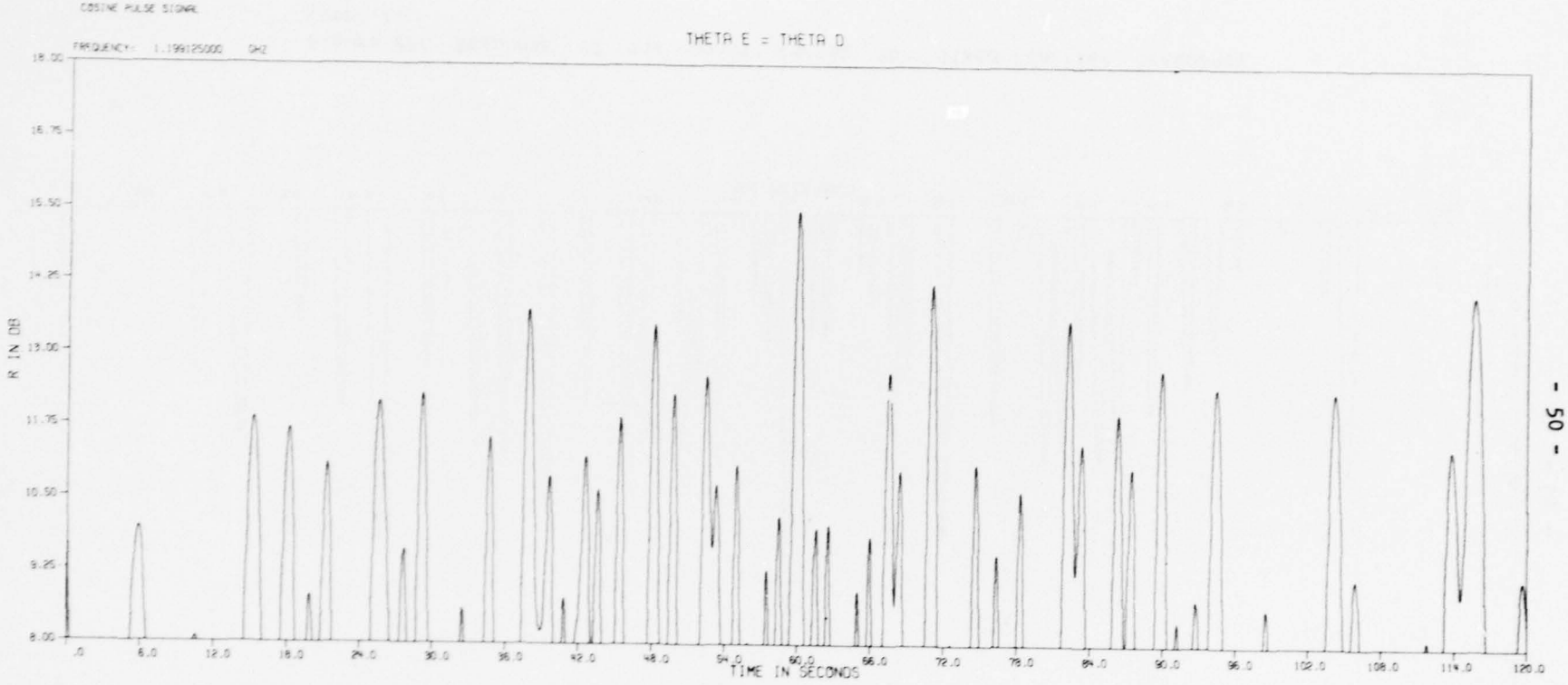

Figure 27d Response of six point target for fixed carrier frequency (cont.).

MISSION
of
Rome Air Development Center

RADC plans and executes research, development, test and selected acquisition programs in support of Command, Control Communications and Intelligence (C^3I) activities. Technical and engineering support within areas of technical competence is provided to ESD Program Offices (POs) and other ESD elements. The principal technical mission areas are communications, electromagnetic guidance and control, surveillance of ground and aerospace objects, intelligence data collection and handling, information system technology, ionospheric propagation, solid state sciences, microwave physics and electronic reliability, maintainability and compatibility.